2017

Numerical Simulation of Multi-Phase Core-Shell Molten Metal Drop Oscillations

Kaushal Sumaria
University of Massachusetts Amherst

NUMERICAL SIMULATION OF MULTI-PHASE CORE-SHELL MOLTEN METAL DROP OSCILLATIONS

A Thesis Presented

by

KAUSHAL JENTI SUMARIA

Submitted to the Graduate School of the
University of Massachusetts Amherst in partial fulfillment
of the requirements for the degree of

MASTER OF SCIENCE IN MECHANICAL ENGINEERING

September 2017

Mechanical and Industrial Engineering

NUMERICAL SIMULATION OF MULTI-PHASE CORE-SHELL MOLTEN METAL DROP OSCILLATIONS

A Thesis Presented

by

KAUSHAL JENTI SUMARIA

Approved as to style and content by:

_____
Jonghyun Lee, Chair

_____
Robert W. Hyers, Member

_____
David P. Schmidt, Member

_____
Sundar Krishnamurty, Department Head
Mechanical and Industrial Engineering

To,

My Parents,
Jenti and Parul Sumaria,
For giving me the wings to fly

My Sister Shailee,
For her love

ACKNOWLEDGMENTS

I would like to express my appreciation to Professor Jonghyun Lee, my advisor, who, through patience and perseverance, has helped me accomplish my goal. I would like to offer my sincere thanks to my thesis committee members Professor Robert W. Hyers and Professor David P. Schmidt for their support and valuable inputs.

I must express my very profound gratitude to my family for providing me with unfailing support and continuous encouragement throughout my life. I would like to thank my friends in Amherst who also became my family away from home. This accomplishment would not have been possible without them. Thank you.

Kaushal Sumaria

ABSTRACT

NUMERICAL SIMULATION OF MULTI-PHASE CORE-SHELL MOLTEN METAL DROP OSCILLATIONS

SEPTEMBER 2017

KAUSHAL J. SUMARIA, B.E., UNIVERSITY OF MUMBAI

M.S.M.E., UNIVERSITY OF MASSACHUSETTS AMHERST

Directed by: Professor Jonghyun Lee

The surface tension of liquid metals is an important and scientifically interesting parameter which affects many metallurgical processes such as casting, welding and melt spinning. Conventional methods for measuring surface tension are difficult to use for molten metals above temperatures of 1000 K. Containerless methods are can be used to measure surface tension of molten metals above 1000 K. Oscillating drop method is one such method where a levitated droplet is allowed to undergo damped oscillations. Using the Rayleigh's theory for the oscillation of force-free inviscid spherical droplets, surface tension and viscosity of the sample can be calculated from oscillation frequency and damping respectively.

In this thesis, a numerical model is developed in ANSYS fluent to simulate the oscillations of molten metal droplet. The Volume of Fluid approach is used for multiphase modelling. The effect of numerical schemes, mesh size, and initialization boundary conditions on the frequency of oscillation and the surface tension of the liquid is studied. The single-phase model predicts the surface tension of zirconium within a range of 13% when compared to the experiment data. The validated single phase model is extended to predict the interfacial tension of a core-shell structured compound drop. We study the effect

of the core and shell orientation at the time of flow initialization. The numerical model we developed predicts the interfacial tension between copper and cobalt within the range of 6.5% when compared to the experimental data. The multiphase model fails to provide any conclusive data for interfacial tension between molten iron and slag.

TABLE OF CONTENTS

Page

LIST OF TABLES

Table Page

LIST OF FIGURES

Figure Page

CHAPTER 1

PROBLEM DEFINITION

1.1 Problem Definition

The surface tension of liquid metals is an important and scientifically interesting parameter which affects many metallurgical processes such as casting, welding and melt spinning. A first principles calculation of the surface tension would require an atomic scale of the liquid state, including density and free-energy profiles at the surface [1]. Conventionally, surface tension measurement for liquids is done using techniques discussed in section 2.1 which measure the geometry of the drop resting on the substrate or measure the pressure required to force out the droplet from end of a capillary. These experimental data are easy to obtain for liquids at temperatures up to 1000 K. However, for metals with high melting point above 1000 K, measurement becomes difficult due to error in measurement of drop profile, error arising from density determination and physio-chemical effects [2]. Therefore, methods need to be explored where these limitations can be compensated and accurate measurements can be achieved. Containerless processing methods such as oscillating drop method (ODM) is one such method [3]. In this method, a sample is levitated using an electrostatic or electromagnetic levitator and allowed to oscillate by providing external excitation, which is removed and sample is allowed to damp out naturally. The oscillating droplet area at successive small time intervals is analyzed and mode 2 natural frequency of the oscillations is obtained. The frequency is used to calculate surface tension [4]. The oscillating drop method is extended to multi-phase core-shell molten metal droplets to study interfacial tension between liquids in core and shell. Systems consisting of molten iron and slag is particularly interesting to study due to its

application in continuous casting process. During continuous casting process, molten iron and slag layer interact at the inlet nozzle. The flow of iron carries slag into molds and affects the quality of the casting. The knowledge of this interfacial tension between molten iron and slag will help predict the behavior at the interaction of iron and slag and help reduce impurities in the casting.

1.2 Summary of This Study

The literature shows that surface tension measurement is critical aspect of processing of materials. The available methods are difficult to use with molten metals at high temperatures in the range of 1500 K and above. ODM was developed and used with levitation to determine the surface tension in a contactless manner thus eliminating difficulties encountered in conventional methods. However, ODM needs extensive setup and controlled environment to successfully process the materials. Computational fluid dynamics (CFD) is a great tool to analyze such problems. A numerical model allows to create conditions close to experiment setup and replicate the physics by solving governing differential equations. This allows to study the effect of various parameters on the outcome of the experiment without the cost of scaled physical setup. CFD studies also help in investigating the problems in extreme environments and validity of assumptions to be used in the scaled model experiments.

The problem of oscillating, levitated drop is controlled by many parameters. For example, the heating of levitated drop is done using a heat source such as laser or magnetic induced electricity. A temperature gradient on the surface of the droplet is developed if the heating is uneven. Secondly, since the sample is levitated and without support from a

physical fixture, a small imbalance in force can result in the rotation of the sample. In the problem of oscillating compound drop formed by core-shell structure, CFD provides insights into the processes happening inside the droplet. The opacity of the molten metal does not allow this in the real-life experiment. Simulating the problem using CFD can help design suitable experiments. Insights can be obtained into various limiting factors of the scaled model experiments.

The aim of this study is to simulate the core-shell structured droplet formed by molten iron core and molten slag as shell. The numerical model is validated using the experiment data available in the literature to gain confidence in the numerical schemes used for numerical simulation. Existing research by Egry *et al.* [5] and Zhao *et al.* [6] provides data from levitation experiments performed on Copper-Cobalt and Zirconium samples respectively. A numerical model is developed to simulate these experiments using Fluent [7] and validated using the experimental data. The validated model is then used to predict the interfacial tension between molten iron and molten slag.

CHAPTER 2

BACKGROUND

2.1 Survey of Experimental Methods for Surface Tension Measurement

Ref. [8] provides a brief description of experimental methods applied for surface tension measurements. It also provides the data obtained using these methods for various materials. A short description of methods along with their advantages and limitations at high temperatures are summarized below.

Sessile drop method is the most popular method to measure surface tension over a wide range of temperatures when compared with other methods that are used at high temperatures. The method measures the geometry of the stationary drop resting on a substrate. The simplicity of mechanical setup and mathematical calculations makes it popular method. However, precaution must be taken to avoid sample contamination.

Maximum bubble pressure method provides fresh sample for each measurement reducing the contamination to minimum. In this method, a capillary is immersed at different depths in a fluid and inert gas is passed through it. The pressure required for the bubble to detach from capillary is measured to find surface tension. Mathematical corrections are needed to compensate for the gravity acting on the bubble.

Pendant drop method and the Drop weight method are similar to the sessile drop method. The shape of a drop hanging from the tip of vertical capillary or rod is measured. The weight of the drop is balanced against forces of gravity to determine surface tension. The rod used is made of same material which eliminates contamination whereas

contamination in the capillary is eliminated by heating the end. These methods are popular for reactive or refractory metals. Limitation of the drop weight method is it can be used to find surface tension only at melting point.

A method similar to maximum bubble pressure method is the Maximum drop pressure method. The pressure required to force a droplet out of upward facing capillary is measured. The method claims to be free of theoretical uncertainty [8]. However, the application of this method is limited to temperatures about 1000 K.

The methods described here are widely used to calculate surface tension of liquid metals. However, the limitations of temperature range and possibility of sample contamination make it difficult to use them for applications in this study. Oscillating drop method described in detail in section 2.3 is suitable for the problem described in this study.

2.2 Containerless Method in Materials Science

High temperature analysis and lab processing of metals and alloys is difficult. There are numerous problems in handling of the sample which arise due to contamination of the sample by chemical reaction with the atmosphere or containers, constant heat transfer due to temperature gradient, evaporation of the sample and mass reduction and consistently maintaining the sample at high temperature etc. To avoid these problems, containerless methods were developed in which the sample does not get in contact with a container. For containerless processing methods, the sample is levitated. This can be achieved by various methods such as electrostatic, electromagnetic, acoustic, aerodynamic or optical forces. The literature reviewed for this study uses electrostatic or electromagnetic levitation. A brief account of these methods is given.

2.2 Survey of Levitation Methods

2.2.1 Electrostatic Levitation

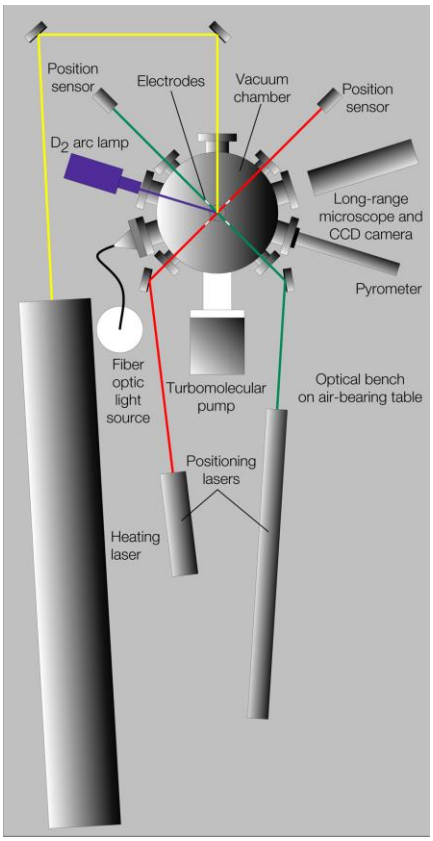

Figure 2.1: Schematic of Electrostatic levitation [9]

Electrostatic levitation (ESL) levitates small samples of approximately 2~3 mm (~40 mg) diameter using a large alternating electric field. The sample is charged by induction. During processing, concept of photoelectric effect is applied using a UV source to refresh the charge on the sample. Therefore, ESL can be used to levitate both conducting and non-conducting samples. Figure 2.1 shows the schematic of the ESL system. The position of the sample is controlled by active feedback control loop, input to which is provided by two dual-axis position detectors. The sample is heated to desired temperature using CO_2, Nd:YAG, or diode lasers. Optical pyrometry provides temperature

measurement required during the containerless processing. Depending on the type of study, the sample is recorded and observed in a video or other suitable means.

2.2.2 Electromagnetic Levitation

The electromagnetic levitation (EML) uses the concept of Lorentz force to levitate and position a sample for containerless processing. An alternating electromagnetic field is used to induce eddy currents in the sample. EML can be used only with conducting samples. Lorentz force is produced due to the interaction of induced eddy currents with the applied magnetic field. By manipulating the applied magnetic field, a non-zero volume integral of Lorentz force is achieved. This net force is used to balance the sample against the gravitational forces. EML setup is used in ground based experiments or microgravity experiments. The ground based EML, vertical magnetic gradient is applied to balance gravity; where as in microgravity conditions, oscillating electromagnetic field is applied.

2.3 Oscillating Drop Method for Surface Tension and Viscosity

The oscillating drop method (ODM) was developed to determine the surface tension and viscosity of the liquid. The basis of ODM is the Rayleigh's theory for surface tension driven oscillations of spherical, force-free and inviscid liquid droplet [4]. The Rayleigh's theory assumes very small amplitude for the oscillation of the droplet. The fluid flow is assumed to be Newtonian, inviscid flow. The ODM needs a form of levitation, electromagnetic or electrostatic to levitate the sample and induce oscillations. The sample oscillations are allowed to damp out naturally. The frequency of oscillation, ω is related to surface tension, σ by the relation given by Lord Rayleigh

$$\omega_0 = \sqrt{\frac{l(l-1)(l+2)\sigma_0}{\rho_0 R_o^3}} \tag{2.1}$$

Where, ω_0 is the oscillating frequency for the mode *l*, for a droplet of surface tension σ_0, density ρ_0, and radius R_0.

For a perfectly spherical, non-rotating drop, only mode 2 oscillations are observed and Equation 2.1 reduces to

$$\omega_0^2 = \frac{8\sigma_0}{\rho_0 R_0^3} \tag{2.2}$$

The viscosity, η of the droplet fluid is related to damping constant, τ of the oscillations by the relation given by H. Lamb.

$$\tau = \frac{(l-1)(2l+1)\eta}{\rho_0 R_0^2} \tag{2.3}$$

where, η is the molecular viscosity if the flow is laminar, or effective viscosity for turbulent or transitional flow [9].

The Rayleigh theory assumes inviscid fluid flow and the equilibrium is governed by surface tension forces. When viscosity is included, the equilibrium state are then governed by the linearized equation of motion [10]. The nonlinear analysis by Suryanarayana *et al.* shows that the surface oscillation depends on parameter α^2 [11],

$$\alpha^2 = \frac{\omega_0 \rho_0 R_0^2}{\eta} = \frac{\sqrt{l(l-1)(l+2)\sigma_0 \rho_0 R_0}}{\eta} \tag{2.4}$$

where ω_0 is the Rayleigh frequency defined in Equation 2.1. For mode 2 oscillations, the critical value of α^2 is 3.69. For the droplet to undergo damped oscillations,

the value of α^2 must be greater than 3.69. For value of α^2 below 3.69, the droplet will exhibit non-periodic oscillations. Suryanarayana *et al.* also tabulated the difference in Rayleigh and observed frequency due to viscous effects. For the value of α^2 greater than 59, the deviation of observed frequency from the Rayleigh frequency is 1% [11]. Therefore, viscous effects can be neglected and Equation 2.1 can be used to compute surface tension from the oscillation frequency of the droplet.

2.3 Oscillating Drop Method for Interfacial Tension

Before extending the containerless, the oscillating drop method to determine surface tension and interfacial tension, it is necessary to know the mechanism that forms core and shell structure between two immiscible liquids. The mechanism of core-shell formation is explained in Ref. [3]. Alloys with metastable miscibility gap can be solidified after undercooling to form a core-shell structured droplet. Below the binodal temperatures, the homogenous melt of alloy undergoes demixing forming small droplets of liquid L1 in the matrix of other liquid L2. The small droplets and matrix must follow compositions per the phase diagrams. The liquids L1 and L2 are not pure; L1 and L2 are rich in components 1 and 2 of the alloy respectively. Initial nucleation kinetics gives rise to large number of small droplets which is energetically non-desirable due to large interface area generated. A diffusive mechanism of Ostwald ripening leads to coarsening of the droplets at expense of small droplets thereby changing the structure and leading to two separated phases. Energy stability of the system dictates the liquid with lower surface tension to form the shell which encapsulates the core formed by liquid with higher surface tension.

Another aspect of interfacial tension measurement experiment using container-less and electromagnetic levitation is to maintain the core-shell structure achieved by undercooling and phase separation. However, the large gradient in magnetic field to balance the droplet against the gravitational forces creates stirring effects, destroying the separated core-shell structure. Since core and shell liquids have different densities, the gravitational force acting on them is not equal. This imbalance can also destroy the core-shell structure. The experiment must be conducted by maintaining the separated core-shell structure and this is possible only if gravitational forces acting on the sample are removed by conducting the experiment in microgravity conditions. Various means used to achieve microgravity conditions are parabolic flights, sounding rockets or in recent times performing experiment in international space station (ISS).

Rayleigh's formula in Equation 2.1 gives relation of surface oscillation to surface tension. Since there are two interfaces, one between liquid L1 and L2, other between liquid L2 and the vacuum, the system will oscillate at two fundamental frequencies: σ_0 attributed to surface tension and σ_{12} attributed to interfacial tension. Work of I. Egry shows ODM can be extended to compound drop formed by immiscible liquids [5]. Based on the theory of Saffren *et al.*[12], analysis for force-free, concentric spherical drops was worked out. The same nomenclature is used here.

$$\omega_{\pm}^2 = K_{\pm}\frac{W}{J} \tag{2.5}$$

where, *K* and *J* are dimensionless, while W is frequency squared. W/J is given by:

$$\frac{W}{J} = \frac{\omega_0^2\tau^8}{\sigma}\frac{1}{(1+\Delta\rho_i)\tau^{10} + \frac{2}{3}\Delta\rho_i} \tag{2.6}$$

where, ω_0 is the Rayleigh unperturbed frequency (Equation 1) of a simple single phase drop with density ρ_0, radius R_0 and surface tension σ_0. Figure 2.1 defines additional symbols along with following equations.

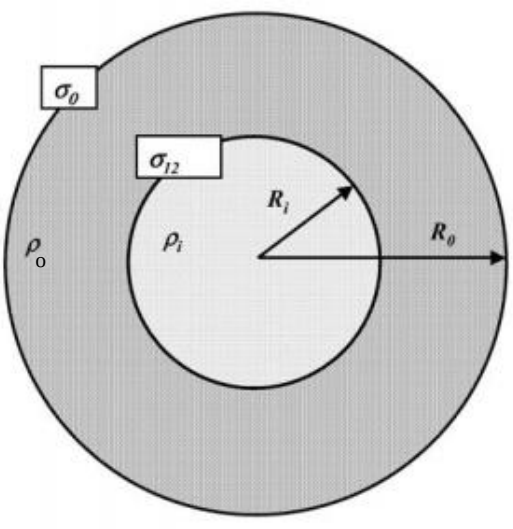

Figure 2.2: A compound drop with core-shell structure

$$\tau = \sqrt{\frac{R_0}{R_i}} \tag{2.7}$$

is the square root of the ratio between outer and inner radius,

$$\sigma = \sqrt{\frac{\sigma_0}{\sigma_{12}}} \tag{2.8}$$

is the square root of the ratio of the surface tension and the interfacial tension, and

$$\Delta\rho_i = \frac{3}{5}\,\frac{\rho_i - \rho_0}{\rho_0} \tag{2.9}$$

is the weighted relative density difference between liquids L1 and liquid L2. Expression for *K* is given by:

$$K_{\pm} = \frac{1}{2}\left(\frac{\sigma m_i}{\tau^3} + \frac{m_0\tau^3}{\sigma}\right) \pm \sqrt{\frac{1}{4}\left(\frac{\sigma m_i}{\tau^3} - \frac{m_0\tau^3}{\sigma}\right)^2 + 1} \tag{2.10}$$

The additional symbols m_0 and m_i are given by:

$$m_0 = \frac{3}{5}\tau^5 + \frac{2}{5}\tau^{-5} \tag{2.11}$$

and,

$$m_i = (1 + \Delta\rho_i)\tau^5 - \Delta\rho_i\tau^{-5} \tag{2.12}$$

for large σ and small $\Delta\rho_i$, approximate equations can be derived for the two frequencies ω_+ and ω_-:

$$\omega_+^2 = \omega_0^2\left(1 + \frac{1}{\sigma^2\tau^4}\right) \tag{2.13}$$

$$\omega_-^2 = \omega_0^2\frac{\tau^6}{\sigma^2}\left(1 - \frac{5}{3}\tau^{-10}\right) \tag{2.14}$$

It is mentioned earlier that gradient in electromagnetic forces used to balance the droplet against gravity in a ground based experiment generate eddy currents in the sample. Conducting the experiment in microgravity can eliminate the requirement for a large gradient in balancing forces.

The levitation methods also report discrepancies in the viscosity measurements with both electromagnetic and electrostatic levitation methods. This is believed to be caused by turbulent flow generated in the sample by the positioning force in electromagnetic levitation and Marangoni flow in electrostatic levitation. [9]. Experiment parameters must be controlled closely to achieve accurate results.

2.4 Literature Review

Researchers have used experiment setup with electromagnetic or electrostatic levitation and ground or microgravity conditions to conduct containerless processing of materials. Ground based oscillating drop experiment were carried out using electromagnetic oscillations by Fraser *et al.* [13] and by Schade *et al.* [14] and Keene *et al*. [15].

I. Egry *et al.* used oscillating drop method on a FeNi sample using thee TEMPUS EML facility. The preliminary results yielded surface tension of 1.6 N/m [1]. The experiments were in excellent agreement with literature which reported the surface tension of FeNi to be in the range of 1.5 – 1.8 N/m. The difference in the observed and the experiment value was attributed to the oxidation on the surface of the sample.

Egry *et al.* extended the oscillating drop method to multiphase, core-shell structured droplets to determine interfacial tension between the materials forming the core and shell *i.e.* copper and cobalt respectively [5]. The experiments were performed in microgravity conditions using TEXAS-EML module onboard the TEXAS-44 campaign. The experiment setup and results are discussed in detail in section 3.2.

Experiments were performed by Hyers *et al.* on Pd-18Si alloy over large range of temperatures [9]. The experiments were carried out onboard a space shuttle in microgravity conditions. The surface tension and viscosity data was collected for many materials such as zirconium and steels. These experiments provided for first time measurement of viscosity using containerless method [9].

In recent times, experiments were performed using ground based electrostatic levitation at Marshall space flight center (MSFC-ESL) by Zhao *et al.* The research was aimed at finding the thermophysical properties of zirconium and effect of oxygen on the surface tension of zirconium. The experiment provides data for the surface tension of pure zirconium obtained by containerless processing which is used to validate the numerical model developed in this study.

Masahito Watanabe performed ODM analysis on compound drops where Ag melts formed the core and B_2O_3 melts formed the shell. The droplets were electromagnetically levitated using a ground based levitator. However, when the sample was melted, the core-shell structure was lost and a Janus droplet was formed [16]. It was concluded that microgravity conditions are required to maintain the core-shell structure [16]. A numerical simulation was also performed on molten iron and slag system to predict the interfacial tension [16].

CHAPTER 3

EXPERIMENTS AND MODEL PARAMETERS

3.1 ODM Experiment to Determine Surface Tension of Zirconium

This section describes the experimental setup and results from containerless processing of zirconium by Zhao *et al.* [6]. A pure zirconium sample was tested using an electrostatic levitator at NASA MSFC. The levitated sample was excited by an electrostatic field alternating near the natural frequency of the sample. A function generator was used to regulate the excitation frequency. After the required excitation was achieved, the function generator was turned off and the sample was allowed to damp freely. The experiment was recorded by high-speed video camera at 1000 frames per second.

The experiment parameters are described here. A vacuum of 10^{-7} Torr was maintained in the equipment chamber. This avoided contamination of sample by elements like oxygen and sulfur. The zirconium sample of mass 43.288 mg was used. Examination of sample after experiment reported a mass loss of 0.043% due to evaporation. The mass loss is neglected in the simulation model. The density of sample was calculated to be 5891.7 Kg/m^3. The sample went through 24 oscillation cycles at temperatures between 1980 ^{0}C and 1600 ^{0}C. The simulations were recorded using LED back light, high speed camera. The video processing was done using code generated in LabVIEW. Surface tension and viscosity data was calculated using relations in section 2.3.

The Fluent model is developed using the density and sample mass used in the experiments. The data from a single oscillation cycle at 1974 ^{0}C is used. The frequency of

surface oscillations was found to be 168.88 hz and surface tension and viscosity for this cycle was calculated to be 1.4515 N/m and 0.0081499 kg/m-s respectively.

3.2 ODM Experiment to Determine Interfacial Tension of Cu-Co Compound Drop

Egry *et al.* conducted experiments to find interfacial tension between Cu-Co using TEXUS-EML during TEXUS-44 campaign. This section provides details of experiment setup and results from experiments described in Ref. [5]. To accommodate the experiments within 160 seconds of microgravity time available for this experiment, the sample was prepared ex situ allowing for phase separation of Cu-Co and formation of core-shell structure. The composition of the sample was $Cu_{75}Co_{25}$.

The physical parameters of the sample must be known for analysis of oscillation spectrum. Theoretical calculations for oscillation of phase-separated drop were done by inputting the physical parameters in Equations 2.4 to 2.14. Sample examination provided total mass of sample to be 1.31 g and mass of individual phases, copper and cobalt to be 1.0056 g and 0.3064 g respectively. The composition of the alloy was calculated to be 76.65 wt% copper and 23.35 wt% cobalt. The radius of the droplet was estimated from the total mass, M which is 1.31 g.

$$R_{eff} = \sqrt[3]{\frac{3M}{4\pi\rho}} \tag{2.15}$$

The density, ρ calculations were done using work of Satio *et al.* [17], [18] and R_{eff} was calculated as 3.475 mm. This is taken as radius of shell R_0. By EDX analysis of identical generated samples, composition of shell liquid, L2 and composition of core liquid, L1 was found to be 90 wt% copper, 10 wt% cobalt and 16 wt% copper, 84 wt% cobalt

respectively. Using this data, the radius of core, R_i is calculated to be 2.149 mm. The surface tension estimates are calculated using models from Ref. [19]. Inserting the physical values in Equation 2.5, theoretical oscillation frequency obtained for a phase separated drop is 28.75 Hz and 17.26 Hz.

Short current pulses were used to excite the sample. The oscillations from the top view of the sample were recorded using a camera recording at 11700 frames per second. Parameters such as radii in prolate and oblate direction, and projected area of the sample from the front view were recorded and area signal was used for further analysis. Three oscillations from the first melting cycle of the phase-separated droplet were obtained and are shown in Figure 3.1 [5].

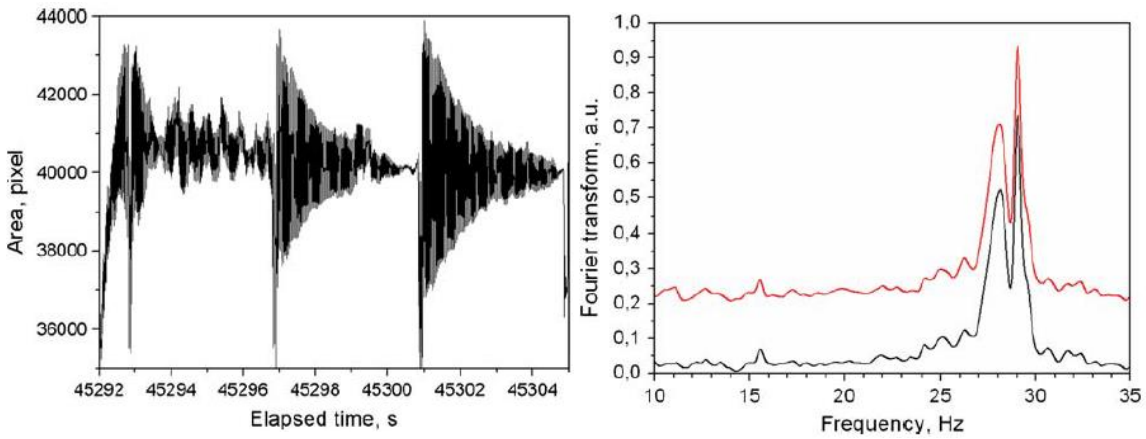

(a) **(b)**

Figure 3.1: (a) Oscillation spectrum and (b) Top - oscillation frequency of projected area of phase separated copper-cobalt droplet [5]

The frequency spectrum in Figure 3.1(b) shows two distinct peaks at 28 and 29 Hz and one individual peak near 15 Hz. It was concluded that the phase separated droplet which was oscillating at 15 Hz and 29 Hz. The oscillation due to heat pulses breaks the equilibrium and the core-shell structure is lost. This forms a homogenized droplet of liquid with composition of 76.5 wt% copper and 35.5 wt% cobalt. It was concluded that the peak

at 28 Hz was due to the oscillation of this homogenized drop. The surface tension, σ_0 and interfacial tension, σ_{12} were then calculated from the experiment data as 1.21 N/m and 0.17 N/m respectively. It should be noted that these data are obtained at temperature of 1863 K.

When comparison is made, the value of interfacial tension obtained from experiments is less than previously estimated by the theoretical calculations. The difference was approximately 0.05 Hz. The reason for this was the compositions of liquids L1 and L2. Precise knowledge of compositions of liquid L1 and L2 was not available and thus theoretical calculations predicted higher interfacial tension. Another possibility that was considered was the homogenization of the droplet. When the droplet is homogenized, the density of the droplet due to compositions of the liquids increases which can have reducing effect on the value of interfacial tension. In summary, uncertainty in the determination of composition data results in discrepancy in interfacial tension values rather than the uncertainty in experiment.

CHAPTER 4

NUMERICAL MODEL AND SOLVER

This chapter discusses the governing equations of the fluid flow and the numerical model used to simulate the oscillations of the droplet. The numerical model is divided into three main sections i.e. Pre-processing, Solving, and Post-processing. These terms are associated with any numerical model used to simulate real life fluid flow problem by method of computational fluid dynamics (CFD). The pre-processing includes making suitable assumptions to simplify the numerical model, setting up the geometry, generating mesh, and applying the suitable boundary conditions. The solver includes details of time and spatial discretization, initializing the problem, and selection of discretization schemes. The post-processing includes interpretation of results from the simulation and documenting the results in form of reports, graphs and contours. The chapter provides insights into methods available along with their advantages and limitations. Subsequently, numerical schemes in this study are described.

4.1 Fluid Flow and Governing Equations

The fluid flow is governed by non-linear set of partial differential equation based on the principle of conservation of mass and momentum. Collectively they are denoted as Navier-Stokes equations. For an incompressible flow, the Navier-Stokes equations are written as,

$$\rho\left[\frac{\partial u}{\partial t} + (u.\nabla)u\right] = -\nabla p + \mu\nabla^2 u + \rho g \tag{4.1}$$

and, the continuity equation,

$$\nabla.u = 0 \tag{4.2}$$

where p is the static pressure, μ is the molecular viscosity, u is the fluid velocity, ρ is the density of fluid, and g is the gravitational force acting on the fluid. The Navier-Stokes equations are non-linear coupled equations and almost impossible to solve for complex problems. To solve such equations, various numerical methods are available some of which are discussed in this chapter.

In CFD, the governing equations are integrated on the individual control volumes to construct algebraic equations for unknows such as convection velocities and pressure. Then discretized equations are then linearized and solution of the system gives updated values of the dependent variables. The linearized equations are solved iteratively until convergence is achieved.

4.2 Pre-Processing

4.2.1 Assumptions

Before CFD study, suitable assumptions were made to simplify the problem. Reasonable assumptions were made such that it simplified the modeling of problem.

The temperature was assumed to be same everywhere in the domain. The temperature gradient on the droplet can cause natural convections and Marangoni convection in addition to the primary fluid flow. In the EML experiments, the primary driving force for the flow is magnetic field. The importance of Marangoni and natural convection was found to be orders of magnitude smaller compared to electromagnetically driven flow [20]. Therefore, its effect on surface tension calculations is neglected. In the ESL experiments, the primary driving force for the fluid flow is Marangoni convection.

The natural convection is found to be very small compared to Marangoni flow in ESL experiment of FeCrNi drops [20]. Therefore from the literature available, it is safe to assume same temperature throughout the domain.

The rotation of the droplet was neglected. The sample is prone to rotation in absence of any fixture support. Even a small imbalance in the forces acting on the levitated sample can cause rotation of the sample. If the sample rotation is below 30 Hz, its effect on surface tension and viscosity can be neglected. However, experiments must be controlled such that the sample does not rotate near its natural frequency which can cause instability due to resonance. If the rotation is considered in the model, a centripetal force term is added to the Navier-Stokes equation.

The droplet is assumed to be spherical always. The levitated droplet experiences gravitational and electromagnetic force at the same time. The net resultant force integrated over the volume is equal to zero. However, there resultant residual forces exist on the surface which deform the droplet. This aspherical shape causes Rayleigh frequency to split into three frequencies. The model is developed such that there are no external forces acting on the drop. Therefore, spherical droplet assumption is valid.

4.2.2 Model Material Properties

A numerical model was developed to simulate the oscillation of pure zirconium (Zr) droplet using the ANSYS Fluent package. The values of various material properties used are given in this sections. The diameter of zirconium droplet modeled was 2.412 mm. The materials used in the model were zirconium for the droplet and helium for the region surrounding the droplet. The values of material properties used for zirconium and helium

are given in Table 4.1. The mass loss of 0.043% due to evaporation was neglected. Density of the sample used was 5891.73 kg/m^3 [6] and working pressure was set to 10^{-7} Torr. The viscosity of zirconium was calculated using empirical model in literature and found to be 4.194 mPa-s [8]. The material properties are summarized in Table 4.1.

Table 4.1: Physical model parameters for Zirconium model

Diameter	2.411E-03 m	
Material properties	Helium	Density: 0.1625 kg/m^3
		Viscosity: 1.99E-05 kg/m-s
	Zirconium	Density: 5891.7 kg/m^3
		Viscosity: 0.004194 kg/m-s
Surface tension modeling	1.451 N/m	

Table 4.1: Physical model parameters for Copper-Cobalt compound drop model

Diameter	Copper (shell)	3.475E-03 m
	Cobalt (core)	2.149E-3 m
Material properties	Copper	Density: 7507.4 kg/kg/m^3
		Viscosity: 0.002012 kg/m-s
	Cobalt	Density: 7618.1 kg/kg/m^3
		Viscosity: 0.004074 kg/m-s
Surface tension modeling	Copper-air	0.21525 N/m
	Copper-cobalt	1.1547 N/m

The model parameters for the copper-cobalt compound drop were obtained from the experiment described in Section 3.2. In the Ref. [5], empirical models for density and viscosity of alloys with varying composition of copper and cobalt are provided. These empirical models were used to calculate the values of required material properties at 1863 K. Table 4.2 summarizes the material properties used for the copper-cobalt compound drop method.

4.2.3 Computational Domain

The geometries are generated in ANSYS Parametric Design Language (APDL). The computational domain for the zirconium droplet oscillations is shown in Figure 4.1(a).

The geometry was set in 2D plane. The problem domain was set in a rectangle of 4 mm width and 2 mm height. The zirconium droplet was generated by a semicircle whose center coincided with the midpoint of lower edge and the horizontal diameter coincided with the bottom edge of rectangular domain. The diameter of the semicircle was 2.4119 mm.

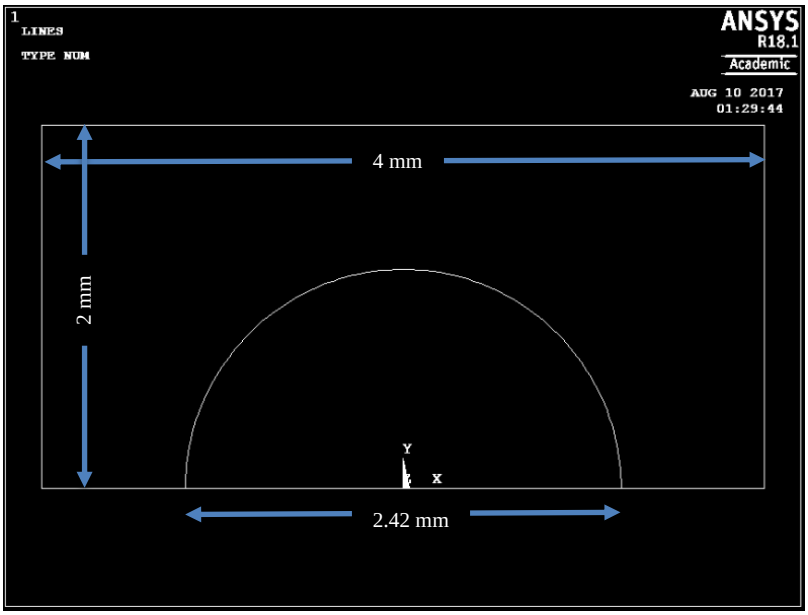

(a)

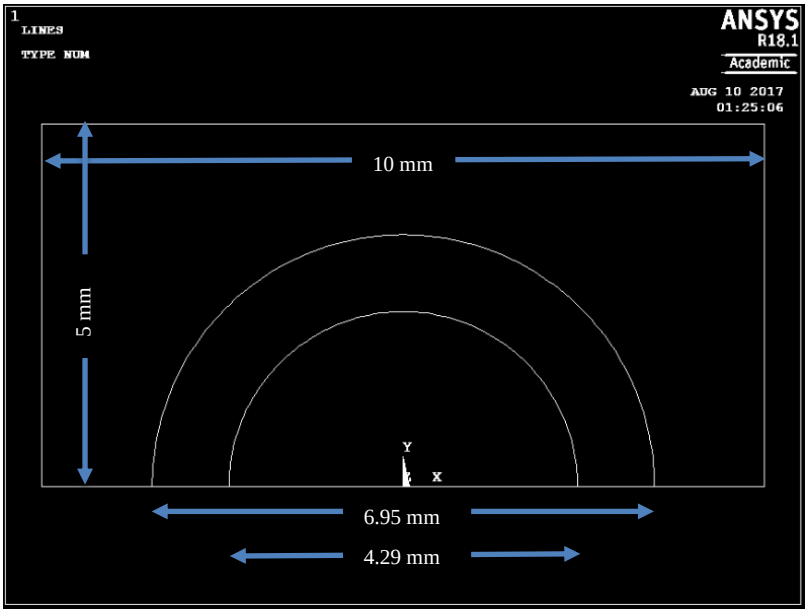

(b)

Figure 4.1: Computational domain and (a) Geometry of Zirconium drop (b) Geometry of Copper-Cobalt compound drop

Figure 4.1(b) shows the computational domain for compound drop oscillation. The geometry was set in 2D plane. The domain was set in a rectangle of 10 mm width and 5 mm height. Two concentric semicircles of diameter 6.950 mm and 4.298 mm were used for copper and cobalt domains respectively. Like the zirconium model described above, the horizontal diameter of semicircles and the center of semicircles coincide with the bottom edge and its center respectively.

4.2.4 Meshing

When solving the fluid flow problem with help of computational methods, the equations of fluid flow are solved at discrete points in the domain. Therefore, the geometry is divided into a large number of smaller areas in 2D or volumes in 3D called cells. The problem in this study was 2D axisymmetric and therefore, a 2D axisymmetric mesh was used. The domain was divided into smaller areas so that the discretized fluid flow equations can be applied to each cell. The mesh was also generated in ANSYS APDL module.

It is important to know the difference between structured and unstructured mesh types. A structured mesh is where each cell is surrounded by equal number of neighboring cells. The cells are orthogonal in i, j in 2D and i, j, k in 3D where i, j, k are the Cartesian axis. Structured meshes in 2D and 3D domains are dominated by quadrilateral and hexahedral elements respectively. Computationally, structured mesh is memory efficient since cells can be numbered using indices and it is easy to develop a code that loops through such an arrangement.

An unstructured mesh does not require each cell to be surrounded by equal number of cells. The arrangement of cells is irregular and is generated by solving an optimization

problem where least number of cells of required size are used to fill the domain. Unstructured meshes are generated using triangular elements in 2D and tetrahedral, or prism elements in 3D domain. With respect to code, node numbers instead of indices are used to denote the cells. The major limitation of structured mesh is difficulty in meshing complex shapes. In such cases a hybrid mesh is used where the regions near complex geometries are meshed in unstructured manner. This reduces the memory requirements and makes the CFD code more efficient.

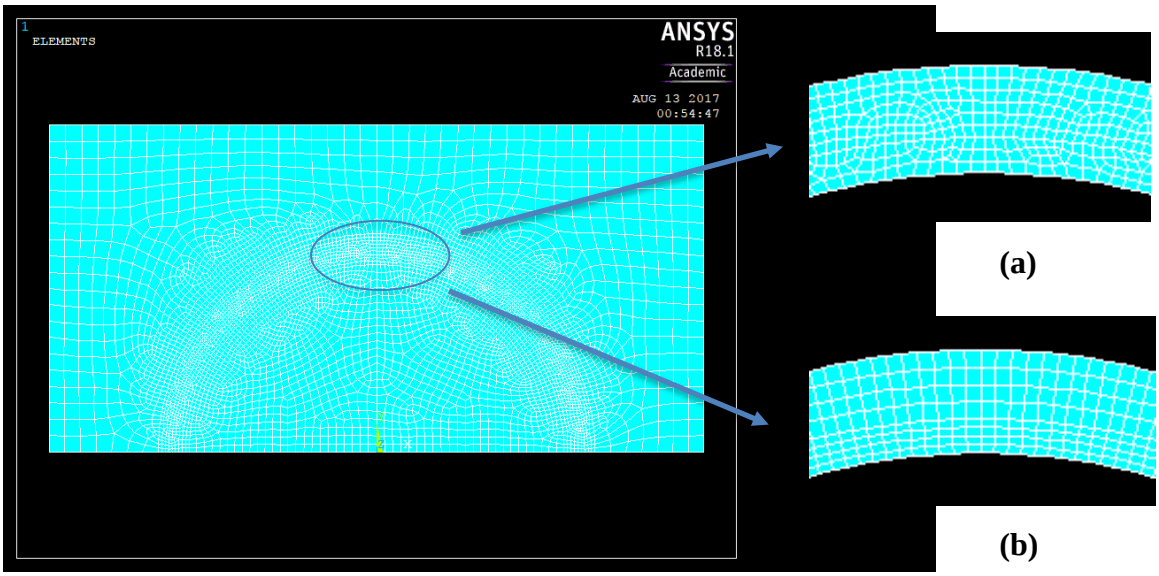

Figure 4.2: (a) Unstructured and (b) Hybrid mesh

For this study, three kinds of meshes were used, A structured mesh, an unstructured mesh, and a hybrid mesh. The element size in interface regions in all meshes used was selected as 12.059 μm for zirconium model and 34.75 μm or 21.49 μm for copper-cobalt multiphase model, which is equal to 1% of the radius. In structured mesh the whole domain was divided into smaller squares of equal dimension. This kind of mesh can be visualized as a Cartesian mesh with rows and columns with each cell being a square of equal dimension. In unstructured mesh, both the regions, interface and bulk, were meshed

without a regular pattern using quads and triangular elements. The mesh generated did not have a regular pattern and consisted minimum number of cells possible while satisfying the dimension constraint. The hybrid mesh was generated such that the interface regions had structured mesh aligned with the curvature while bulk regions had unstructured mesh. The mesh generated had quad cells arranged in a regular pattern in the interface region and quads and triangular elements arranged in an irregular pattern in the bulk region.

4.2.5 Boundary Conditions

The boundary conditions are an important part of pre-processing of a CFD problem. The two vertical side edges and top edge of the computational domain were set as wall. The velocity component normal to walls was set as zero and the velocity component tangential to the wall was set equal to the velocity of the wall. The velocity of viscous fluid assumed 'no-slip' conditions at the axis. The droplet was modeled using a 2D axisymmetric model. Therefore, the bottom edge was assigned axis boundary conditions. A zero-flux condition normal to the axis was also applied as a part of axis boundary condition.

4.2.6 Initialization

The problem was initialized by assigning each cell with a value for volume fraction of zirconium. As per geometry, the cells which lie outside the droplet were initialized with volume fraction 1 for helium phase and 0 for zirconium phase. Similarly, the cells within the droplet were initialized with volume fraction 1 for zirconium phase and 0 for helium phase. The droplet was provided with a perturbation in the form of an ellipticity. The ellipticity value used was between 1% and 5% with respect to radius of the droplet. An user defined function was developed in 'c' to perform the initialization.

4.3 Numerical Modeling and schemes

This section describes the schemes used for discretization and solution of the governing equations described in Section 4.1.

4.3.1 Multiphase Modeling

The Fluent provides Volume of fluid (VOF), Level set, Eulerian and Mixture models for multiphase modeling. This section describes these methods as well as the multiphase modeling approach used in this study.

The VOF model uses a Eulerian approach to model multi-phase flows. The phase interfaces or boundaries are modeled using a variable F. Consider the flow of single-fluid system. The variable F has positive value between 0 and 1 for a cell which contains fluid whereas, for an empty cell, the value of F is zero. In a multi-phase system, each phase is assigned the variable F and its value within each cell will indicate an relative amount of fluid(s) present in cell. For example, a non-zero value of F_1 within a cell means fluid 1 is present in cell in ratio of F_1 with respect to total fluid in the cell. For a system with two phases, the cell containing the interface will have non-zero F value for both the phases. For cells that do not contain an interface or boundary, the value of F_1 or F_2 will be 1 which means the cell is occupied by only single fluid. The summation of variable F for all the phases should be equal to 1 for a cell. While solving the discretized equations of fluid flow, a single momentum equation for all phases is solved. The properties of individual phases are a function of variable F and global property.

The level set model provided in Fluent tracks the boundary of interface instead of phase distribution. The boundary is represented by closed curve using an auxiliary

function. The shape of curve changes when the function is evaluated at different values. Computationally, the Mixture model is similar to VOF model since a single momentum equation is solved for the mixture phase. However, it is different from VOF model in two aspects. Firstly, the phases can be interpenetrable and secondly, phases are allowed to move at different velocities. This model can be used for modeling problem where one phase is dispersed in matrix of second phase. The Eulerian model allows modeling of multiple phases in solid, liquid or gaseous state. However, the model is limited by convergence behavior. The simulation also needs an initial solution to begin the simulation.

In this study, Volume of fluid modeling was used. VOF modeling allowed to track the interface which was very important in our study. The post processing technique for the same is explained in Section 4.4**.** While implementing the VOF scheme, both explicit and implicit volume fraction formulation were used. Theoretically, explicit formulation is known to exhibit better accuracy compared to implicit formulation. However, explicit formulation is bounded by the value of time step. The time step must satisfy the Courant-Friedrichs-Lewy (CFL) condition. For this study a velocity based CFL condition is used. The CFL condition provides acceptable time steps which are calculated using volume of fluid v_f, mesh size Δx, and courant number *C*. The Courant number was set between 0.1 and 0.25 for various cases. The acceptable time step value is given by,

$$\Delta t = \frac{C\Delta x}{v_f} \tag{4.3}$$

To satisfy the above condition, time step values between $1x10^{-5}$ s and $1x10^{-7}$ s were used. Implicit volume fraction scheme formulation provides unconditional stability for any

time step used. However, the time step size is limited by truncation error. Therefore, for all implicit formulation cases, the time step of $1x10^{-6}$ s was used.

4.3.2 Time Discretization

In an unsteady or transient problem, the plow properties such as pressure and velocity change in the space domain and time domain. The rate at which properties change with respect to time is calculated at small, successive time steps. The flow properties at later time steps are approximated by first order implicit scheme. The information about flow properties at times other than the time steps is not available. Depending on the case setup, time step values between $1x10^{-5}$ s and $1x10^{-7}$ s were used in this study. These time steps were chosen by trial and error method to satisfy the CFL condition. A generic information for evolution of property ϕ over time is given by [7]

$$\frac{\partial \phi}{\partial t} = F(\phi) \tag{4.4}$$

In first order, implicit formulation, the $F(\phi)$ is calculated at future time step, [7]

$$\frac{\phi^{n+1}-\phi^{n}}{\Delta t} = F(\phi^{n+1}) \tag{4.5}$$

The Equation 4.4 is solved iteratively before moving to the next time step. The maximum number of iterations allowed to reach convergence was set to 100. Again, by trial and error method it was found that 100 iterations per time step were enough to converge the residuals at each time step.

A second criterion along with CFL condition for free surface numerical stability is developed in Ref. [23]. The momentum normal to the surface is critical for the stability and is considered in the formulation of the criterion. The surface waves driven by the surface

tension are generated on the free surface. These are known as capillary waves and travel at speed, *c*, and depend on the wavelength of disturbance λ

$$c = \sqrt{\frac{2\pi\sigma}{\rho\lambda}} \tag{4.16}$$

The value of λ is taken approximately same as mesh resolution. Thus, by the capillary wave criterion, the surface will be stable for an appropriate explicit scheme when

$$\Delta t < C\sqrt{\frac{\rho\Delta x^3}{2\pi\sigma}} \tag{4.17}$$

In the Equation 4.7, C is of order unity and depends on the numerical method.

4.3.3 Spatial Discretization

In a CFD analysis values of the fluid properties are calculated and updated after each time step. To make the code memory efficient, the fluid properties are evaluated only at the center of the cells in the domain. However, the discretized fluid flow equations given in Equation 4.1 and 4.2 contain flux terms where transfer of fluid properties through cell faces are evaluated. In order to obtain the value of fluid properties at the face, extrapolations schemes are used and value of fluid properties at cell faces are estimated. The discretization schemes used for calculating gradients, pressure and momentum at cell faces, and volume fraction interpolation are explained in this section.

PRESTO! (PREssure STaggering Option) scheme was used for the pressure interpolation. Pressure at cell faces is needed to discretize the momentum equation. In PRESTO!, the pressure is calculated at cell faces rather than interpolating from cell centers.

This is done using discrete continuity balance across the face of a control volume. This study used structured mesh with VOF multiphase modeling in a curved domain, hence, PRESTO! is an easy choice. An unstructured mesh is also used for this study, however, PRESTO! achieves similar accuracy for unstructured mesh. The PRESTO! scheme provides high accuracy however, the scheme is computationally expensive, since flow information at more than one location in a control volume is stored.

Quadratic Upwind Interpolation (QUICK) scheme was used to interpolate velocity at cell faces. QUICK scheme is a third order scheme and based on weighted average of second order upwind and central interpolation schemes. When QUICK scheme is used with hybrid meshes, QUICK scheme will be applied on the hexahedral or quad cells aligned with fluid flow and second order scheme will be used for the triangular or hex cells.

When the fluid interface is critical for study, donor acceptor schemes are not suitable since a smooth interface is not generated. The Geo-reconstruct scheme was used to generate interface when using explicit VOF formulation. The geo reconstruct scheme generates the interface using piecewise linear approach where interface between two fluids has linear slope as shown in Figure 4.3. When using implicit VOF formulation, geo-reconstruct scheme was not available. Therefore, as per the suggestions in Ref. [7], the modified HRIC scheme was used.

Pressure Implicit with Splitting of Operators (PISO) scheme was used for pressure-velocity coupling. As the name suggests, it is an implicit method and an improvement over predictor-corrector algorithms such as SIMPLE (Semi-Implicit Method for Pressure Linked Equations). PISO is a two-step predictor-corrector scheme. A guessed pressure

field is used to solve the discretized momentum equations and get velocity components. However, these velocity components will not satisfy continuity unless pressure is correct. The first corrector step is to find a correct velocity field using the continuity equation. Further using the corrected velocities and continuity equation, a pressure corrector term is calculated. These steps are used in both the SIMPLE and PISO algorithm. PISO used one more pressure corrector step and enhances the SIMPLE procedure. The corrected pressure field is used with discretized momentum equations and twice-corrected velocity field is obtained. A second pressure correction term is yielded by subtracting the discretized momentum equation obtained by using twice-corrected velocity and single-corrected velocity. Then finally twice-corrected velocity terms are used with continuity equation to get pressure correction equation. PISO was also used because it is stable even with larger time steps.

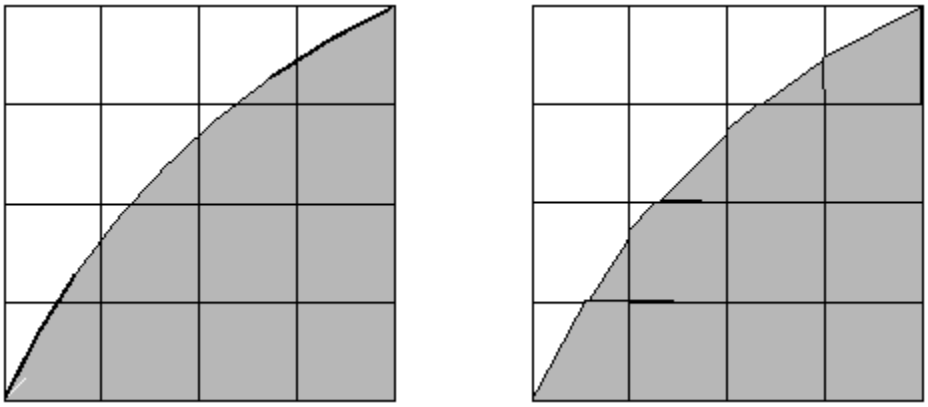

(a) **(b)**

Figure 4.3: (a) The curved boundary of a phase and (b) Piecewise linear approximation using geo-reconstruct scheme

Least cell square based method was used to calculate gradients in the numerical simulation. This method was selected because it is the most accurate method available in Fluent with competent computational time compared to other methods available.

4.4 Post-Processing

A two-step post-processing approach was used. An animation was created which showed the amount of volume fraction of all phases in all cells of the domain at every time step. The generated video was analyzed using code developed in MATLAB. A loop was run where each frame of the animation sequence was analyzed at a time. In experiments, the projected area of the droplet is used to plot the surface oscillations. In the animation sequence, each phase is represented by a color. When analyzing each frame, the number of pixels that lie in each phase is counted. The number of pixels of required phase at all time steps was stored in a variable which is a 1-dimensional array in MATLAB. The number of pixels in a phase and time are plotted on Y and X axis respectively and the oscillation spectrum of the droplet was generated. Further to extract the frequency of oscillation, a fast Fourier transform was performed on the data. In the frequency spectrum, a sharp peak was observed at the frequency of oscillation. The resolution of frequency axis is controlled by the sampling frequency and the number of data points used. For this study, the sampling frequency and number of data points were such that a very coarse frequency spectrum was achieved, which induced an approximation error of 5% to 30% in the predicted oscillation frequency.

In this study, experimental data are used to validate our numerical model. Therefore, the desired value of frequency is known. If the approximate value from the animation sequence was close to data experiment data, a second analysis was performed. The LabVIEW module was used for the area processing of the droplet. A .histo file was generated which contained the histogram of each frame from the animation sequence. This .histo file was then provided as an input to LabVIEW module. The LabVIEW module

filtered the data and a fit to the data was generated using 'Levenberg-Marquardt' method. This method provided the frequency of oscillation accurate to 1/100 Hz. The fit also provided the damping constant which was used to calculate the viscosity of the droplet fluid.

CHAPTER 5

SIMULATIONS, RESULTS AND DISCUSSION

5.1 Zirconium Single Phase model

5.1.1 Modeling for Surface tension of Zirconium

A general strategy used in this study is explained. For each case, the simulation was run for a small flow time of 0.0173 s, enough to capture approximately 3 oscillation cycles. The post processing of the animation sequence was done using the method explained in Section 4.4 and oscillation spectrum was generated. A fast Fourier transform operation was performed on the oscillation data and an approximate oscillation frequency was obtained. This frequency spectrum was of very coarse resolution approximately 56 Hz. The approximate frequency, oscillation spectrum, and the animation allows to make decisions on the feasibility and physics of the model. If the preliminary results showed that the model followed the physics and the numerical model predicted the oscillation frequency correctly, the simulation was run for a larger flow time such that steady state was reached.

Cases were simulated with an unstructured and a Cartesian mesh (Ref. Section 4.2.4 for grid terminology) with an element size 25 μm. The element size is approximately 2% of the radius of the droplet. In order to initiate the oscillations, the spherical droplet was given a perturbation. This was done by giving an ellipticity to the droplet i.e. squeezing it from one direction. This configuration where the droplet diameter between the poles is greater than the droplet diameter at equator is called as prolate. The Equations 5.1 and 5.2 were used to calculate the dimensions of droplet's major and minor axis after accounting

for the ellipticity. The equations are formulated such that the total volume of the droplet remains constant.

Let,
$$e = \frac{a-b}{a}, \therefore b = (1-e)a \tag{5.1}$$

For volume to remain equal,

$$\frac{4\pi}{3}r^3 = \frac{4\pi}{3}a^2 b, \therefore a = \frac{r}{\sqrt[3]{(1-e)}} \tag{5.2}$$

where, r is the unperturbed radius of the droplet, e is the ellipticity and a, b is the major and minor axes of the ellipse. The ellipticity of 5% was used therefore the mesh resolution was enough to capture the oscillations. Cases with these meshes were modeled using the explicit volume fraction formulation. Oscillation spectra from post processing of these cases are shown in Figure 5.1

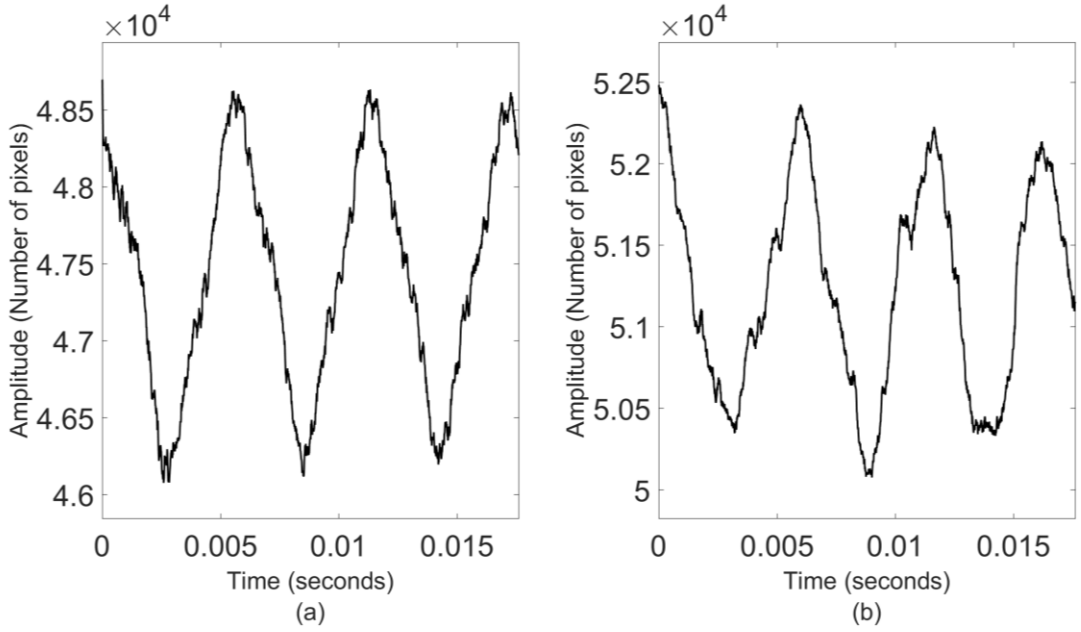

Figure 5.1: Oscillation spectrum for case of 5% ellipticity using (a) Cartesian and (b) Unstructured mesh having element of size 25 µm

Comparison between oscillation spectrum for the Cartesian and unstructured mesh shows that the quality of oscillation spectra for Cartesian mesh was superior to unstructured mesh. The spectrum for both the cases shows noise due to localized surface oscillations. Oscillation spectrum for the Cartesian mesh exhibits clean oscillations at peaks and valleys i.e. when droplets changes the configuration from prolate to oblate and vice-versa. Therefore, Cartesian mesh was used for further analysis in this study.

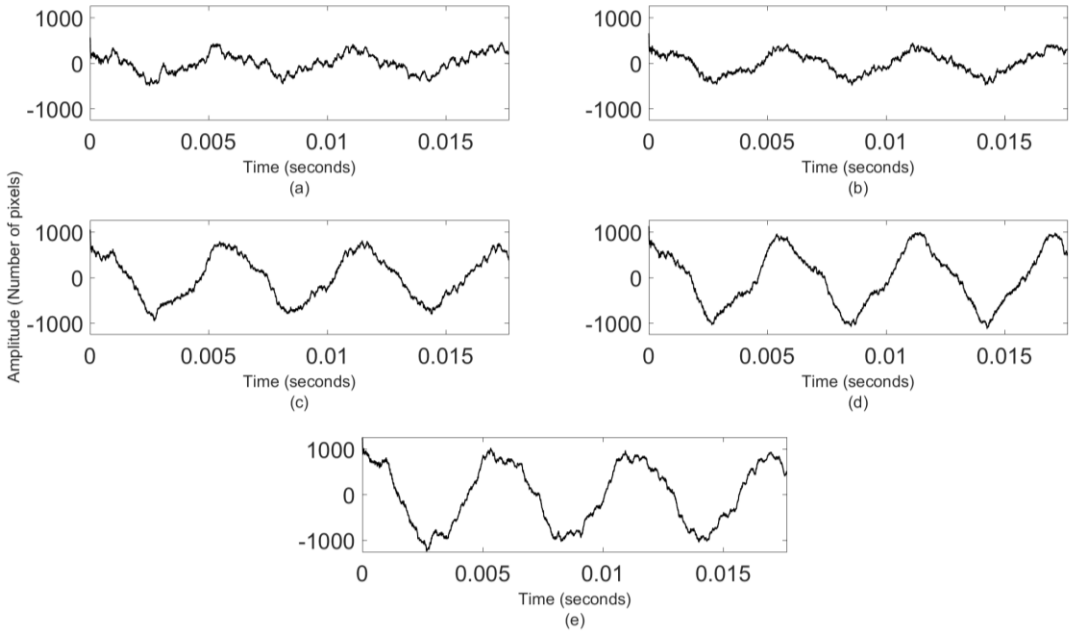

Figure 5.2: Study of effect of ellipticity provided to the droplet of the oscillation of the droplet: (a) 1%, (b) 2%, (c) 3%, (d) 4%, and (e) 5%

To reduce the existing localized surface oscillations, the Cartesian mesh was further refined by using element of size 20 μm which is approximately 1.5% of the radius. The effects of initial deformation on the droplet oscillations and the oscillation frequency was studied. Cases were setup by varying the ellipticity value between 1% to 5%. Figures 5.2(a) to (e) show the oscillation spectrum obtained for these cases. The Figures 5.2(a) and (b) show the presence of high frequency surface oscillations. For ellipticity of 3%, 4%, and 5%, the spectrum is relatively clear of surface oscillations. However, the Figures 5.2(c) and

(d) show irregular behavior near flow time of 0.003 s. The oscillation data for case of 5% ellipticity was found to be clean of noise but with irregularities. For further cases, 5% ellipticity is used to perturb the droplet from equilibrium and initialize the flow.

The study of initial deformation shows the presence of noise in the oscillation spectrum for all five cases. The noise to signal ratio varies but noise was prominently seen in the low ellipticity case. It was necessary to remove any source of noise due to localized surface oscillation at high frequency. From the literature provided in Ref. [7], it was clear that the surface tension force modeling method induced this noise in the oscillation spectrum. In the modeling terminology, these high frequency surface oscillations are called parasitic currents. Fluent provides two methods, continuum surface force (CSF) and continuum surface stress (CSS) for surface tension force modeling. Both methods will induce parasitic currents due to imbalance of pressure gradient and surface tension force. Ref. [7] also shows that the calculation of surface tension is not accurate on the triangular elements. This agrees with the result shown in Figure 5.1(b), where an unstructured mesh containing triangular elements was used. A detailed explanation of modeling using these methods is given in Ref. [7].

To choose a surface tension modeling method, cases were run using both CSF and CSS methods. The cases were set up with zero ellipticity i.e. without disturbing the equilibrium. The idea was to maintain the droplet equilibrium and allow the simulation to calculate only the parasitic currents. Since the droplet is already in the equilibrium, the surface tension forces should not cause any droplet or surface oscillations and any oscillations generated will be result of numerical formulation of these methods. Figure 5.3 shows the surface oscillations generated when using CSF and CSS methods. The parasitic

currents generated in both the methods were of approximately equal magnitude. CSF and CSS were the only methods in Fluent for surface tension force modeling. Further in this section, the formulation of CSF is explained. It was understood that by making the interface smooth, the parasitic currents can be controlled. Therefore, it was decided to use CSF method for all further simulations.

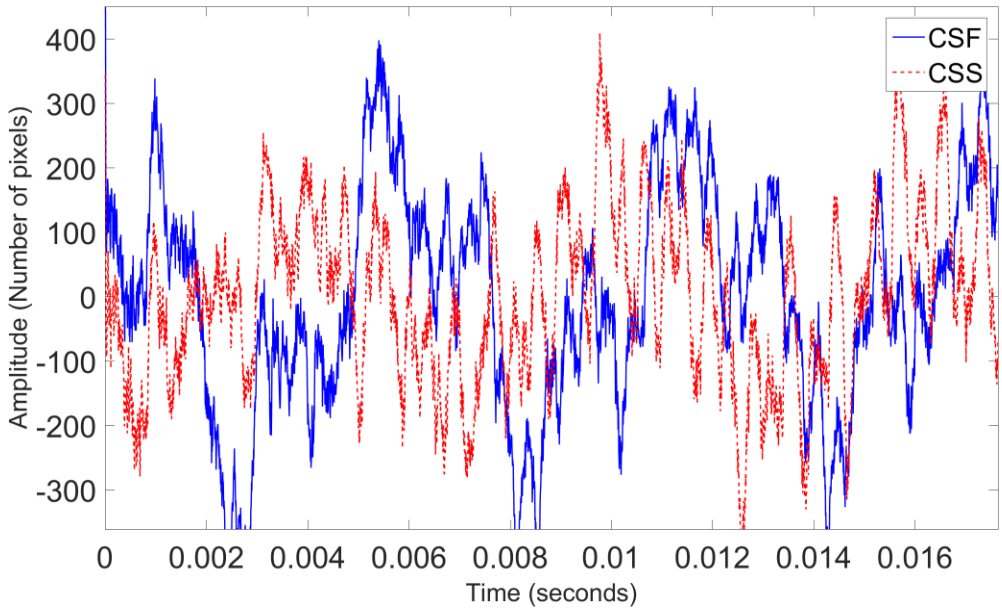

Figure 5.3: Parasitic currents induced due to CSF and CSS formulation

Cases were run to study any improvement in the droplet oscillation spectrum by further mesh refinement. Two cases were set up with mesh size of 10 µm, 20 µm, 30 µm, 40 µm, and 50 µm. The animation sequence for cases with 30 µm, 40 µm, and 50 µm show that coarser interface was generated after initialization and as the flow progressed, the high frequency surface oscillations were increased. Therefore, results from those cases are not discussed further. 10 µm and 20 µm cases were allowed to run for larger flow time such that the droplet is allowed to damp out naturally and reach the steady state. The oscillation spectrum for both the cases are shown in Figure 5.4 and 5.5. It was seen that refining the

mesh did not improve the solution. On the other hand, the case with 20 µm mesh showed a very clean oscillation spectrum. The frequency analysis done using LabVIEW provided the frequency to be ~175 Hz which was close to the experimental value of 168.88 Hz. However, the animation sequence generated shows that the droplet undergoes translation motion along the axis. The case setup did not include any external resultant forces in the direction parallel to the axis. It was concluded that the imbalance in the forces was generated due to the CSF method.

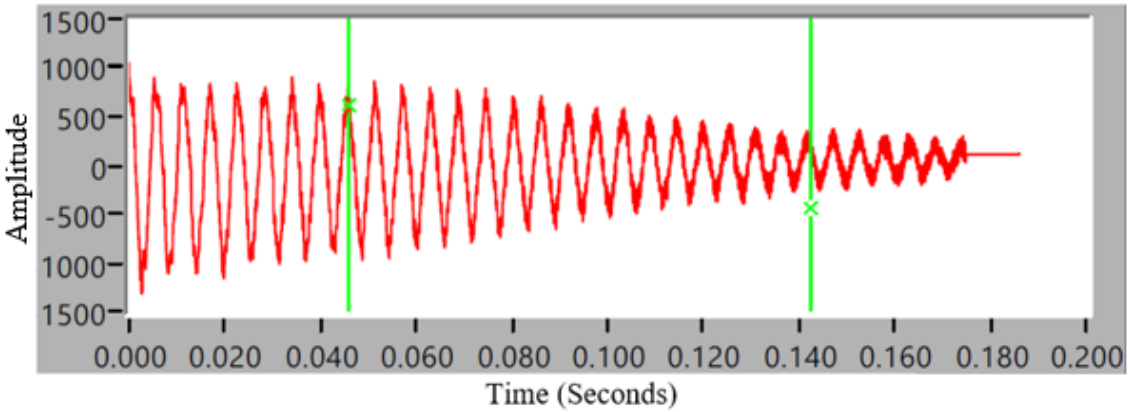

Figure 5.4: Oscillation spectrum for explicit volume fraction formulation on 20 µm Cartesian mesh

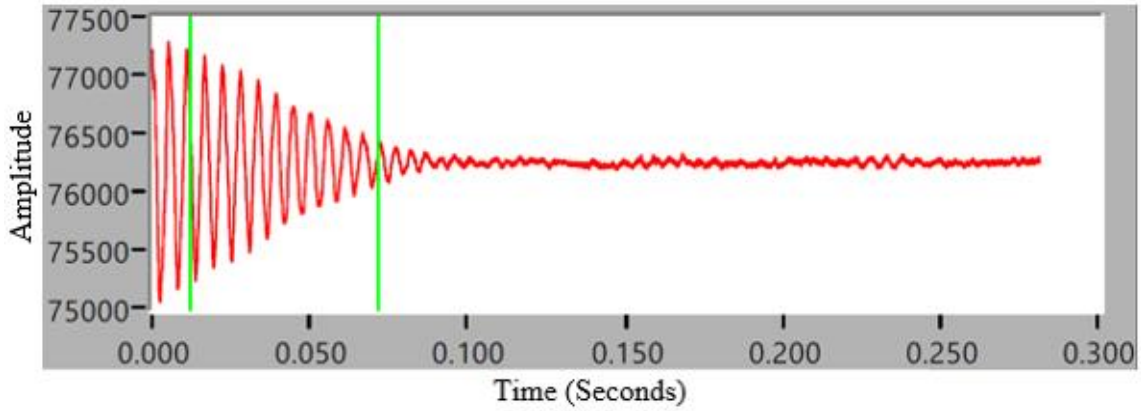

Figure 5.5: Oscillation spectrum for explicit volume fraction formulation on 10 µm Cartesian mesh

A brief understanding of CSF formulation is necessary at this stage. The CSF method computes the curvature from the local gradients in the surface normal at the interface. The surface normal is defined as the gradient of volume fraction. When the

droplet is initialized in fluent, the geo-reconstruct scheme uses piecewise linear interpolation and forms the droplet surface which does not always have an outward normal in radial direction. It can be skewed in direction. Further this surface normal is used to calculate the curvature which will also not be perpendicular to radius of the droplet. Therefore, the surface tension forces modeled will not act exclusively in the radial direction. The unbalanced forces in x-direction accumulate as the flow time progresses and grow in magnitude. This unbalance force causes the translation of the droplet. There are two ways to avoid this. Firstly, use a fine mesh so that the accuracy of piecewise linear approximation improves and unbalanced forces are reduced. Secondly, use a lower ellipticity so that the volume fraction gradient at the interface cells is low. However, results discussed in the above section show that cases with finer mesh or lower initial deformation were not feasible.

The study of Cartesian mesh shows that the interface formed during the initialization resulted in imbalance of forces acting on the droplet. Therefore, a mesh had to be developed where the advantages of structured mesh were retained and the droplet was initialized with a smooth interface. A hybrid mesh was generated where the zirconium-helium interface, the zirconium droplet and helium phase were divided into three sections. The interface was meshed with a structured mesh which followed the curvature of the droplet. Other regions in the mesh were meshed with quad or triangular elements without constraints. The case was set up with the hybrid mesh. However, diffusion observed at the ends of the diameter and the droplet exploded.

Cases were setup using hybrid mesh and implicit volume fraction formulation. The element size of 12 μm which is approximately 1% of the drop radius was selected. This

element size was selected so that it can capture the droplet oscillations when ellipticity of 1% is used. Cases were setup with initial deformation of 1%, 2%, 3% 4% and 5%.

The figure 5.6(a) through (d) shows the oscillation spectrum generated. It is seen that in all cases, the oscillations are damped out and steady state is reached. For the case of 2%, 3%, 4% and 5%, the frequency of oscillation was found to be in the range of 300 Hz. The model overestimates the frequency. For the case of 1% initial oscillation, however, the frequency was found to be 179 Hz. Further mesh refinement did not improve the solution.

A set of cases were set up using the Cartesian mesh and implicit volume fraction formulation. The droplet was initialized with the deformation between 1% and 5%. The frequency analysis of the oscillation spectrum for these cases showed that the model underestimated the frequency of oscillation. The oscillation frequency for the mentioned set of simulation setup was found to be in range of 115 Hz to 130 Hz.

The oscillation frequency predicted by cases run on Cartesian mesh and hybrid mesh using explicit and implicit methods are summarized in table 5.1. The explicit formulation on hybrid mesh and implicit formulation on the Cartesian mesh yielded results which are not in agreement with the experimental data.

The oscillation frequencies predicted by the models in Table 5.1 are well in agreement with the experimental data. The numerical error in the simulation results is less than 10%. The explicit and implicit volume fraction models in combination of Cartesian mesh and hybrid mesh respectively were found to be good enough to predict the oscillation frequency of the zirconium droplet.

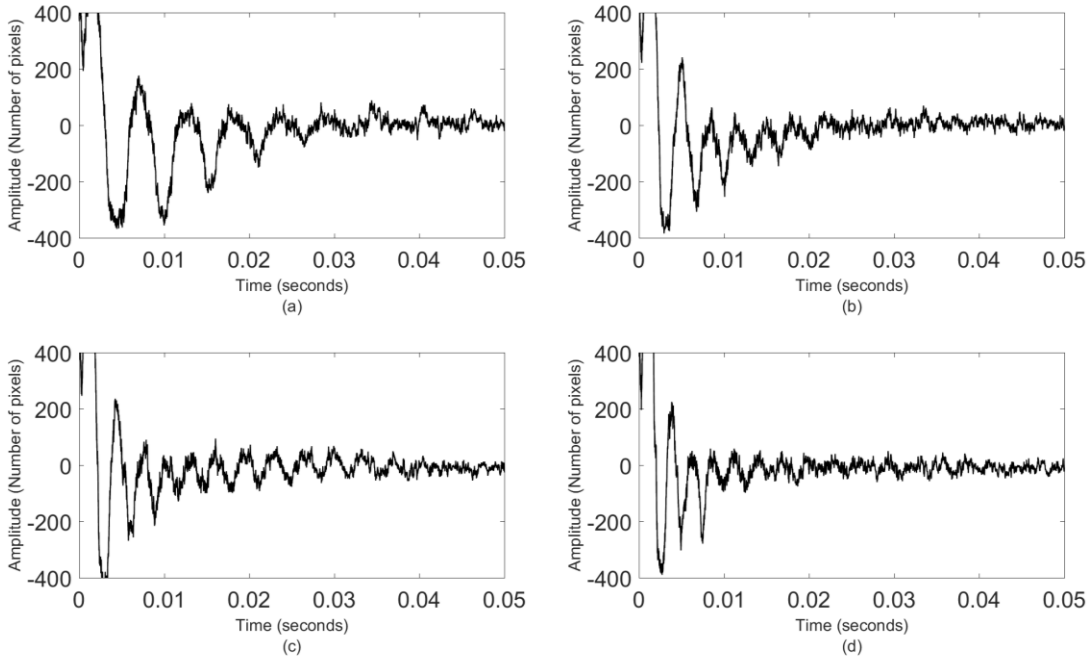

Figure 5.6: Oscillation spectrum generated from Hybrid mesh using implicit volume fraction formulation and initial deformation of (a) 1%, (b) 3%, (c) 4%, and (d)5%

Table 5.1: Summary of results for numerical simulation of Oscillating Zirconium droplet

VOF formulation	Mesh Type	Mesh element size	Initial deformation	Oscillation frequency, Hz	Surface tension, N/m
Experiment	-	-	7%	168.88	1.4515
Explicit	Cartesian	20 µm	5%	174.77	1.5583
Implicit	Hybrid	12 µm	1%	179.11	1.6366

The explicit formulation on the Cartesian mesh was found to be sensitive to initial deformation used to initialize the problem. The reason for this was the noise generated by CSF method due to coarse interface. This also resulted in the translation of the droplet because of the residual forces accumulated in the formulation of CSF method. However, using the mesh of 20 µm provided enough oscillation data for post processing and calculating the oscillation frequency. When a coarse mesh was used, the residual forces are accumulated in a short time and in higher magnitude causing the droplet to bump against

the wall and explode in quicker times compared to 20 μm mesh. Mesh refinement did not improve the outcome. The initial deformation study and mesh study show that 5% initial deformation used with 20 μm mesh accurately predicts the oscillation frequency of the zirconium drop.

The model with implicit volume fraction formulation on the hybrid mesh reached the steady state very quickly compared to the explicit formulation. The implicit formulation on the Cartesian mesh was also found to be sensitive to initial deformation used to initialize the problem. The higher initial deformation caused the model to overestimate the frequency of oscillation. Implicit formulation on the Cartesian mesh was also found sensitive to initial deformation. The quality of the oscillation spectrum improved with increment in initial deformation of the droplet. However, the model underestimates the oscillation frequency. The implicit formulation was unable to simulate the transient flow accurately for higher initial deformation cases.

An important parameter to discuss is the maximum deformation sample undergoes in the experiment and numerical model. The Rayleigh's frequency is based on the linear theory and assumes small perturbations. However, oscillation spectrum generated from the experiment of oscillating droplet show that the maximum ellipticity of the sample at the beginning of the experiment was approximately 7%. For determining the frequency spectrum, a portion of the signal with maximum deformation of approximately few percentages was used. The droplet undergoes damped oscillations and exhibits a single oscillation frequency. Therefore, for comparison purpose, the simulation was performed with the initial deformation similar to that in the experiment

5.1.2 Modeling the damping constant for Zirconium

The oscillation spectrum is also used to get the damping constant of the oscillation. The damping constant is then used with Equation 2.3 to get the viscosity of the liquid. In this study, the viscosity of Zirconium obtained from the Ref. [8], i.e. 0.00419 kg/m-s is used. The idea is to check if the numerical model returns the similar value of viscosity back from the model. The oscillation spectrum for the shown in Figure 5.4 and 5.6(a) are used to calculate viscosity of the zirconium. The calculations are summarized in the table below.

Table 5.2: Summary of results for numerical simulation of Oscillating Zirconium droplet

VOF formulation	Mesh Type	Mesh element size	Initial deformation	Damping constant, 1/s	Apparent Viscosity, kg/m-s
Input value	-	-	~7%	-	0.0041
Explicit	Cartesian	20 μm	5%	0.061	0.02
Implicit	Hybrid	12 μm	1%	0.009	0.18

The results from the viscosity analysis show that the values returned by the numerical model are higher by couple of orders of magnitude. The numerical model fails to account for viscosity in the model.

The possible explanation for this is the simplicity of the numerical model. Viscosity of a liquid is a temperature dependent property. Also, the source of viscosity is the interaction between the molecules of the liquid which is unaccounted for in the model. Therefore, the model fails to accurately predict the viscosity of the molten zirconium.

5.2 Copper-Cobalt Homogenized Drop Model

Ref. [5] explained that during the experiment, the Cu-Co compound drop was homogenized during the experiment. The oscillations of this homogenized droplet are

similar to oscillation of a zirconium model. Cases were setup using the explicit volume fraction formulation on Cartesian mesh and implicit volume fraction formulation on the hybrid mesh. The mesh size and initial deformation used were same as the zirconium model. The material properties for the homogenized phase were calculated from composition mentioned in Ref. [5]. The Figure 5.7 and 5.8 show the oscillation spectrum obtained from these two simulations.

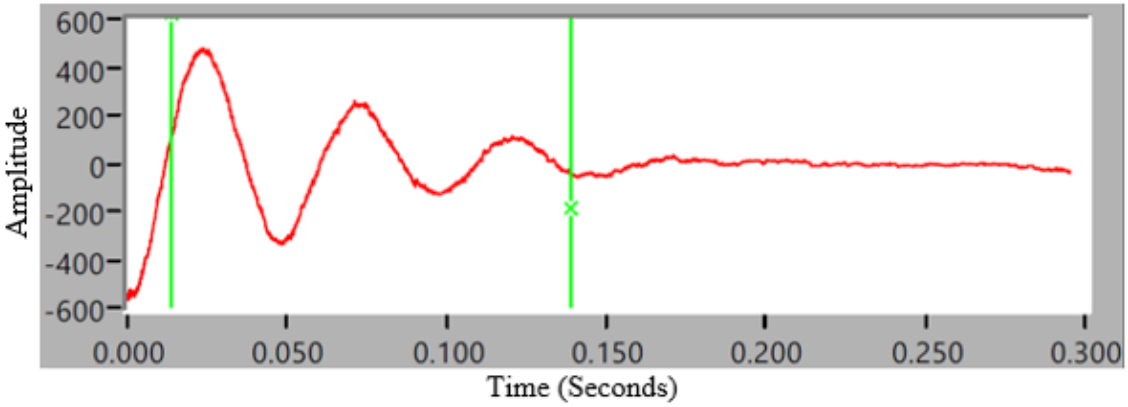

Figure 5.7: Oscillation spectrum generated for homogenized Cu-Co droplet using Cartesian mesh

Figure 5.7 shows the oscillation spectrum for the homogenized Cu-Co droplet obtained by using the Cartesian mesh. The post-processing of the oscillation signal returns the oscillation frequency of 20.93 Hz. The frequency predicted by the model is in the range of 25% compared to experimental data.

Figure 5.8 shows the oscillation spectrum for the homogenized Cu-Co droplet obtained by using the hybrid mesh. After post-processing, the oscillation frequency of 24.65 Hz was obtained which is close to the experiment value of 28 Hz. The model predicts the frequency for simulated model within the range of 13% compared to the experimental result.

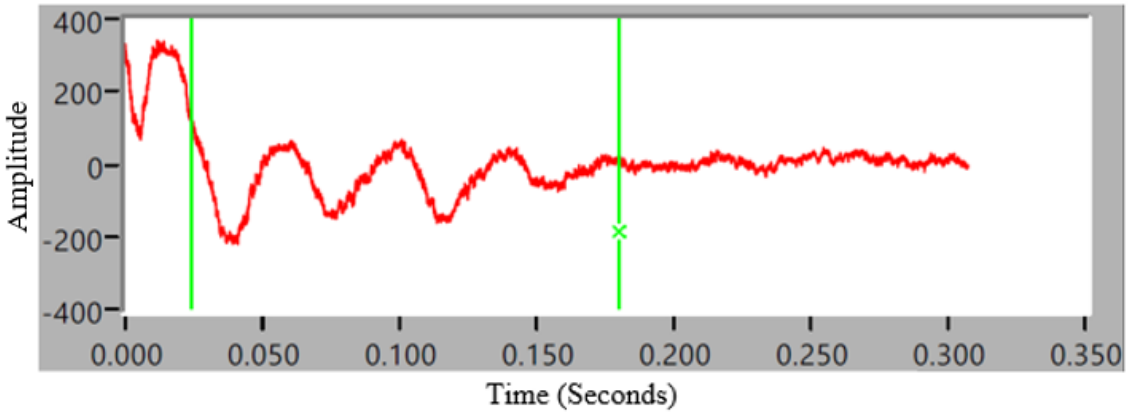

Figure 5.8: Oscillation spectrum generated for homogenized Cu-Co droplet using hybrid mesh

The comparison of results returned by both the simulation cases shows that contrary to zirconium model, the frequencies predicted for homogenized Cu-Co model were further away from those observed in the experiments. Both the simulation cases underestimate the oscillation frequency.

5.3 Copper-Cobalt Core-Shell Compound drop

The single-phase model was extended to core-shell structured droplet shown in Figure 2.2. The mesh size used for the simulation was maintained at 20 µm. The initial deformation used to initialize the flow was 5%. Cases were set up using explicit and implicit volume fraction schemes on Cartesian mesh and hybrid mesh respectively. The advantage of a CFD study for oscillation of compound drop is that it allows to observe the behavior of the core. For both the meshes, two cases each were set up where the core-shell deformation was initialized in phase or out of phase. In phase configuration is one in which the prolate and oblate for both core and shell droplet are in same direction, X in this case. Similarly, out of phase configuration is where the shell is initialized with prolate in X direction and core is initialized with oblate in X direction.

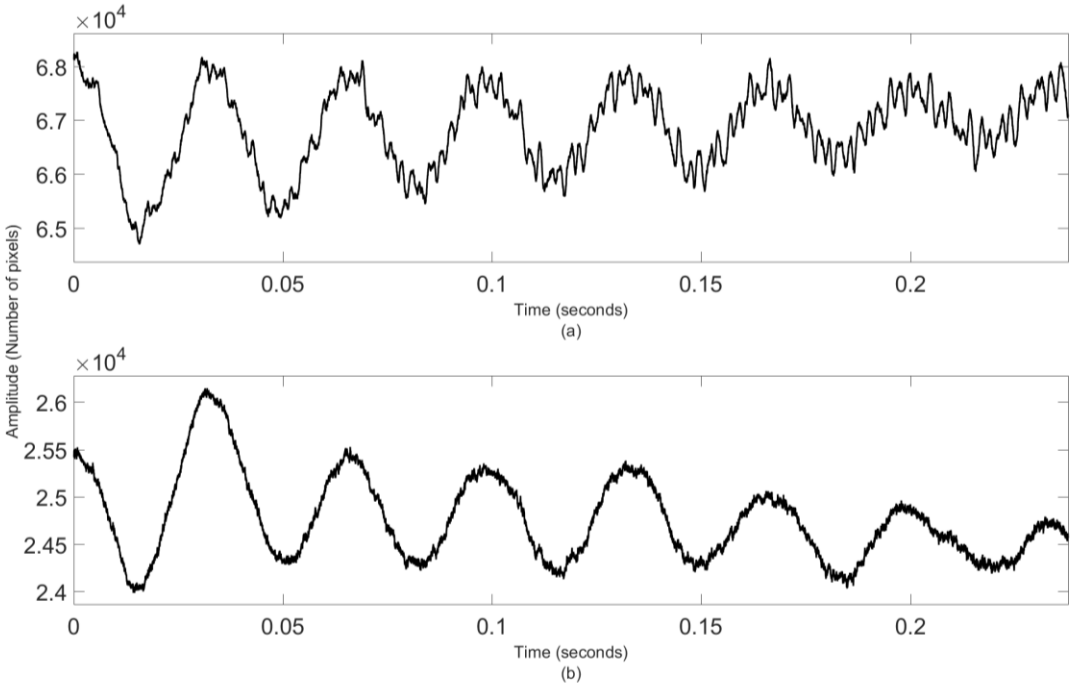

Figure 5.9: Oscillation spectrum for compound drop (top) and the core (bottom) generated by explicit volume fraction formulation on Cartesian mesh and in phase initialization

Figure 5.9 shows the oscillation spectrum for in phase initialization case for model with explicit volume fraction formulation on a Cartesian mesh. From the Section 3.2, we know that for a compound drop, there drop oscillations exhibit two oscillation frequencies. Post processing of the signal revealed the shell oscillates at single frequency of approximately 30 Hz. This contradicts the experiment results. Further, the compound droplet was initialized with out of phase configuration. The Figure 5.10 shows oscillation spectrum for out of phase compound drop.

The post processing of the shell spectrum shows that the droplet oscillates at two frequencies of 14.52 Hz and 29.85 Hz. The intensity of peaks for the 14.52 Hz was approximately 15% of that for 29.85 Hz. The core oscillation frequency also revealed two peaks at these frequencies very close to 14.52 Hz and 29.85 Hz. The small difference in the peaks is neglected. The dominant frequency for the core was ~15 Hz. In figure 5.7 and

5.8, it is seen that the shell oscillation signal contains high amount of surface oscillations and its magnitude increases as the flow progresses.

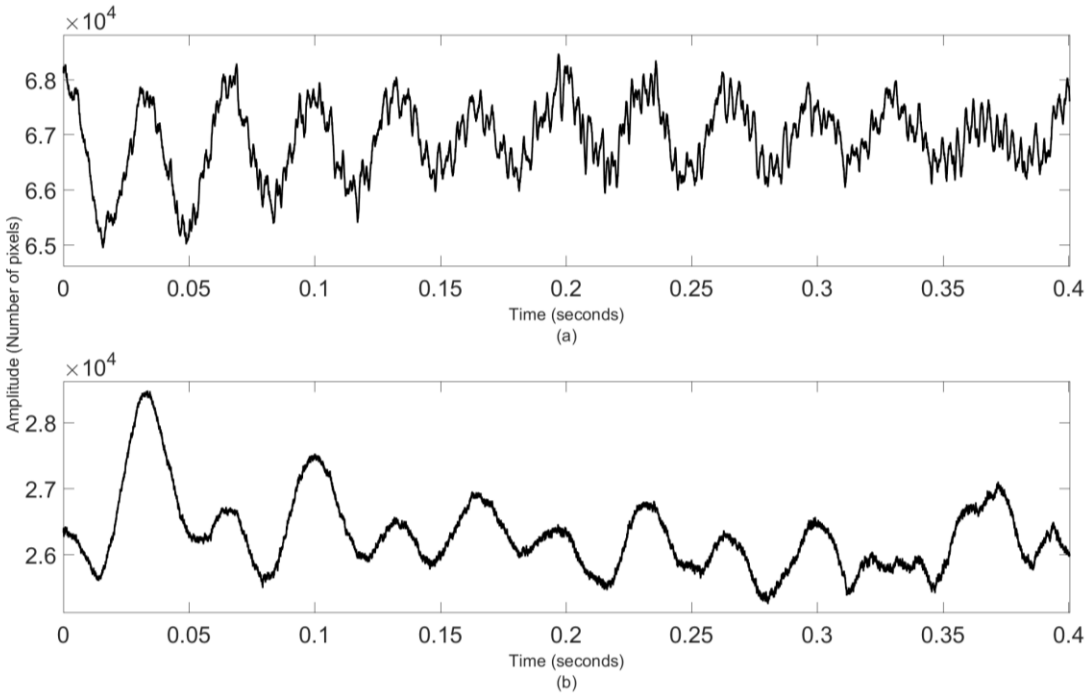

Figure 5.10: Oscillation spectrum for compound drop (top) and the core (bottom) generated by explicit volume fraction formulation on Cartesian mesh and out of phase initialization

The cases with implicit volume fraction formulation on hybrid mesh failed to generate clear oscillation spectrum. The effect of initial deformation and mesh size needs to be investigated further for hybrid mesh.

5.4 Iron-Slag Core-Shell Compound Drop

From section 5.3, it is known that explicit formulation on Cartesian mesh accurately predicted the oscillation frequency and corresponding surface or interfacial tension. Therefore, in this study only explicit volume fraction formulation on Cartesian mesh was extended to predict the interfacial tension between iron and molten slag. The material properties were taken from Ref. [16]. The mesh size and initial deformation of 25 μm and

5% respectively were used. The post processing of the animation sequence shows that no oscillations were obtained. When the flow time progressed, the droplet initialized with ellipticity returns to the spherical shape and continues to remain in that state. The initial deformation could not generate enough forces to initiate oscillations.

The density of molten iron used in the model is approximately three times the density of slag. Also, the viscosity of slag is approximately four time the viscosity of molten iron. The material properties of Cu and Co used in the multiphase model were very close within the range 10%. This can be a reason for inability of the validated multiphase model to generate any oscillations when used for iron-slag compound drop. The modeling strategy needs to be reinvestigated to accommodate large difference in the material properties of iron and slag.

5.5 Summary

The results from the various simulation cases are summarized in this section. Various cases were setup and simulated by varying the mesh, numerical schemes, and initialization conditions.

The explicit volume fraction formulation on a Cartesian mesh is used to simulate the oscillations of zirconium droplet. To keep the model comparable with the experiment, the initial oscillation of 5% was selected for the study. Effects of initial deformation on the oscillation frequency were studied.

Further, mesh dependency was studied. The animation sequence and oscillation spectrum show that for mesh element size greater than 20 μm, the interface generated is

coarse. The VOF model used in this study is a diffusive-interface scheme [21]. The interface boundary is smoothed over 2-3 cells. Therefore, as the mesh size increases, the interface width also increases. Ideally, the droplet surface should be a perfectly smooth curve which is not obtained due to coarse mesh. This causes localized high frequency oscillations at the surface of the drop. It was also observed that the droplet translated in the domain due to unbalanced forces acting on it. It was concluded that the unbalanced forces were generated due to the formulation of CSF method for surface tension modeling. The mesh refinement study showed that refining the mesh below 20 μm did not improve the results. Therefore, initial deformation of 5% and mesh size of 20 μm were used for case setup. The result predicted the surface tension of zirconium as 1.55 N/m which was within the range of 7.5% from the experiment data. A hybrid mesh was developed where the mesh was curved to match the interface curvature and a smooth interface was obtained. However, the numerical model overestimated the frequency of oscillations.

Further, implicit volume fraction formulation on a hybrid mesh was used to simulate the problem. Cases set up with Cartesian mesh underestimated the oscillation frequency in the range of 120 Hz. The hybrid mesh initialized with 1% initial deformation predicted the surface tension within the range of 13% of the experiment data. Higher values of initial deformation used for initializing the flow over estimated the oscillation frequency to approximately 300 Hz. Table 5.1 summarizes the results obtained from the CFD simulation of the oscillating zirconium drop.

The single-phase model is also used to simulate the homogenized droplet which is formed in the later stages of experiments described in Section 3.2 and Ref. [5]. The

numerical model predicts the surface tension within the range of 26% of the experiment data for implicit formulation and 13% for the explicit formulation.

The validated numerical models were extended to simulate the Cu-Co compound drop. The implicit volume fraction formulation on hybrid mesh failed to simulate the problem and provided inconclusive results. The case of explicit formulation on the Cartesian mesh and out of phase initialization accurately predicted the oscillation frequency and surface tension within 6.5% of the experiment data.

The validated multiphase model was used to predict the interfacial tension between the molten iron and slag. The model however fails to provide any conclusive data. Modeling strategy needs to be reinvestigated to accommodate the large difference in the material properties of iron and slag.

5.6 Discussion

This section discusses the results obtained by simulating the oscillating droplet under the influence of surface tension forces in this study and those obtained by previous attempts made by researchers using similar or different techniques. It is important to know that in this study, the decisions on the quality of the solution were made by comparing the numerical solution to the experimental data available as mentioned in Chapter 3. However, the model needs to be verified for multiple materials and dimensions in order for the model to be used universally.

The work of Berry, S. in 1998 attempted simulation of fluid flow in electromagnetically levitated droplets [22]. In the thesis, it is described that calculated electromagnetic force due to positioning coils and heating coils was calculated and

included in the Navier-Stokes to initiate the fluid flow. However, in the current model, external force was not modelled. To initiate the fluid flow, the droplet was initialized with a deformed shape. The mesh used for numerical study by Berry was a curvilinear mesh where the mesh coincided with the curvature of the droplet. The mesh with 60 x 60 elements was used with 30 x 30 elements in the droplet region. A hyperbolic tangent function was used to bias the grid points towards free surface. Total 3600 elements were used. In the current model, a non-curvilinear mesh is used with 20000 square shaped elements distributed uniformly in the rectangular domain. Both the models have used VOF model for the simulations. Berry's model calculated the surface tension to be 70% less than the input value to the model whereas the Cartesian mesh used in the current model calculated the surface tension within 8% of the input value. It can be observed that mesh refinement contributes towards improvement in the numerical simulation results.

It was observed that in zirconium model, mesh refinement alone was not helpful. The mesh refinement resulted in the reduction in the thickness of the interface. However, mesh refinement did not eliminate the high frequency surface oscillations at the poles of the droplet. A stability criterion for high speed capillary waves developed at free surface flows is developed in Ref. [23]. For the case of 20 μm Cartesian mesh the time step of $5\ x\ 10^{-6}$ s used satisfied the constraint for the allowable time step. The constraint on the time-step is in addition to the CFL condition when PISO scheme is used. However, in future study, it must be made sure than the time step satisfies both the CFL and surface waves constraints.

In this study, The VOF method was used to track the interface between the two phases. However, the VOF method is an diffuse-interface scheme [21]. In diffuse-interface

scheme, a fixed grid is used to solve Navier-Stokes equations and the jumps across the fluid properties in the phases are smoothed in the interface. A Eulerian fixed mesh is used in the current study. A piecewise linear interpolation method was used in the cells containing the interface to define phase boundary. A direct interface tracking method is introduced in Ref. [23]. In this method, the region of the mesh containing the interface is deformed at each time step to match the interface resulting in a smooth interface removing the error generated in the regeneration of the interface. The bulk of the phase is meshed using fixed Eulerian mesh and remains undeformed. The direct interface tracking method was applied to simulate flow in a 2-phase incompressible oscillating droplet and the results were in good agreement with the experiments and were documented in Ref. [21]. This method must be explored with the current model to remove the surface oscillations observed at the poles.

Another hypothesis for the oscillations near the poles is the error generated when regenerating the interface boundary near the axisymmetric axis. An alternative to continuum surface force formulation may be required at the poles. One possible approach is to model constant force based on the equilibrium droplet shape near the poles. Another approach to solve this problem is to develop a 3D model which does not contain an axisymmetric axis. However, 3-D flows are computationally expensive.

During the simulation, it was observed that the droplet translated in x-direction. The reason for this is described in section 5.1.1. A subroutine to correct this problem could be developed in the Fluent to introduce a time-dependent body force based on the relative position of the droplet with respect to the dimensions of the domain. Alternatively, a

surface tension evaluation method described in Ref. [24], which is conservative in nature, could be explored to avoid translation of droplet.

In the current model, the viscosity returned by the simulation was found to be 5 times the value given to the model. The research by Berry, S. documented in Ref. [22] shows that turbulent eddy viscosity led to 12 times increment in the molecular viscosity calculated by the simulation. However, since Berry's study used RNG turbulence model, the results from the current and previous viscosity study may or may not be related. It can be hypothesized that the eddy currents generated in the form of surface oscillations in current model provide additional damping and generate the error in viscosity calculations. Ref. [21] shows that using moving mesh interface tracking approach with a 3-D model can accurately calculate the molecular viscosity in a oscillating 2-phase incompressible droplet.

The current model improves the accuracy of the numerical model compared to Ref. [22]. The surface tension returned in their model was 70% less than the input value. The current model calculated the surface tension for a zirconium which is 8% more than experimental value.

CHAPTER 6

FUTURE WORK

The single-phase model developed in this study calculated the surface tension within 8% of the input value. The viscosity calculated from the simulations was found to be 5 times the value provided to the model. Also, the extended multi-phase model calculated the interfacial tension between copper and cobalt within 4% of the experimental data. However, it was found that the problem of high frequency surface oscillations is not handled by the model. The model needs to be improved in that regard and possibilities for the same are discussed in this section.

In the current model, the difference between material properties of phases across the interface is in the order of 10^4. This difference introduces numerical error in the calculations near the interface regions. In order to reduce the error, the second phase can be replaced by a dummy phase with density closer to, perhaps approximately one-tenth of, the droplet density. The reduction in calculation error may stabilize the surface oscillations.

In the Ref. [23], a moving-mesh tracking method is described. This method eliminated the error due to smearing of interfaces in the volume of fluid method. Also, Ref. [24] describes formulation of a surface tension forces which are conservative in nature. Ref. [21] shows application of mesh tracking method to the simulation of incompressible oscillating droplet. These methods must be incorporated in the model in future to improve the simulation results. Also, the use of 3-D model can contribute in error in surface tension modelling near the poles and this option must be further explored.

Modeling correct damping time for a given viscosity is an important part of numerical simulation of ODM and improvement is needed in the current model to accurately calculate it. In the current model the damping time calculated by the model is found to be approximately 5 times less than predicted, corresponding to a viscosity about 5 times greater the value given to the model. Previous work by Quan *et al*. shows that accurate numerical modelling of damping time is possible [21]. In Quan's model, a moving-mesh interface tracking method was used to track the interface boundary between the droplet and surrounding gas. Comparison between the current model and Quan's model shows that existence of surface waves may cause additional damping, in turn causing the model to overestimate the viscosity. Methods to achieve better numerical stability on the surface to be applied to the current model to improve the accuracy of the predicted damping. Quan's work documented in Ref. [21] can provide additional guidance in this regard.

Ref. [16] shows the results from the numerical simulations of iron-slag compound drop. The Ref. [16] shows the numerically predicted interfacial tension between the phases which were in good agreement with the analytical calculations. However, the model developed in this study could not generate any oscillations of the compound drop. The material properties used in both the models were exactly same. Further study needs to be done to find the difference in modelling approach in both the models.

APPENDIX

SIMULATION AND POST-PTROCESSING CODES

ANSYS JOURNAL FILE

```
;Single phase droplet
;SCALE THE MESH
/mesh/scale 1000 1000
;
;SELECT PRESSURE-BASED, TRANSIENT AND AXISYMMETRIC SOLVER
/define/models/axisymmetric yes
/define/models/solver/pressure-based yes
;
;FOR VOF, VOLUME FRACTION IMPLICIT
/define/models/multiphase/model vof implicit 1e-6
;order is  implicit volume-fraction-cutoff
;
;FOR VOF, VOLUME FRACTION ECPLICIT
;define/models/multiphase vof explicit 0.25 no 1e-6
;order is explicit courant-number solve-vof-every-iteration volume-fraction-cutoff
;
;DEFINE NUMBER OF PHASES
/define/models/multiphase/number-of-phases 2
;
;DEFINE MATERIAL PROPERTIES (density kg/m^3, viscosity kg/m-s)
/define/materials/change-create/air helium yes constant 0.1625 no no yes constant 1.99e-
5 no no no yes
/define/materials/change-create/helium zirconium yes constant 5891.73 no no yes
constant 0.004194 no no no no
;
;DEFINE PHASES
/define/phases/phase-domain/phase-1 helium no
/define/phases/phase-domain/phase-2 zirconium yes zirconium
;
;DEFINE DOMAIN INTERACTION
/define/phases/interaction-domain 0 yes yes no no yes constant 1.4515 no
;
;DEFINE SOLUTION METHODS
;define pressure velocity coupling
/solve/set/p-v-coupling 22 ;for piso
;define spatial discretization
/solve/set/gradient-scheme no yes
/solve/set/discretization-scheme/pressure 14 ; 14 for PRESTO!
/solve/set/discritization-scheme/mom 4 ; 4 for QUICK
/solve/set/discritization-scheme/mp 16 ; 16 for Geo-Reconstruct ; 5 for Modified HRIC
```

```
;define transient formulation
;/define/models/unsteady-1st-order yes ;default
;
;INITIALIZE THE FLOW
/define/user-defined/interpreted-functions "UDF_Zirconium.c" "cpp" 10000 n
/define/user-defined/function-hooks/initialization "custom_init_function"
/solve/initialize/initialize-flow
;
;DEFINE ANIMATION SEQUENCE
/solve/animate/define/define-monitor "sequence-1" 2 yes no 10 contour hmf "storage
path"
;
;DEFINE TIME-STEP, ITERATIONS AND FLOW TIME
/solve/set/time-step 1e-6
/solve/set/max-iterations-per-time-step 100
;
;SETUP THE RECORDING AND VIDEO
;
;SOLVE
/solve/dual-time-iterate 1000000 100
```

USER DEFINED FUNCTION FOR INITIALIZATION

```
#include "udf.h"

/*domain pointer passed by INIT function is mixture domain*/
DEFINE_INIT(five_percent_init_function, mixture_domain)
{
        FILE *fp;
        //FILE *fp1;
        int count = 0;
        int phase_domain_index=2;   /*Phase domain index for zicronium*/
        cell_t cell;
        Thread *cell_thread;
        Domain *subdomain;
   real xc[ND_ND];
        int cell_number=1;

   /*loop over all subdomain(phases) in the superdomain(mixture)*/
   sub_domain_loop(subdomain,mixture_domain,phase_domain_index)
   {
        /*loop if secondary phase=zicronium*/
        if(DOMAIN_ID(subdomain)==3)
                {
                /*loop over all cell threads in the secondary phase domain*/
        thread_loop_c(cell_thread, subdomain)
```

```
        {
          /*loop over all cells in secondary phase cell threads*/
          begin_c_loop_all(cell,cell_thread)
          {
                C_CENTROID(xc,cell,cell_thread);
                        if
((pow(xc[0],2.)/pow(0.001226695,2))+(pow(xc[1],2.)/pow(0.001165361,2))<1.)
                        //if ((pow((xc[0]-(-
0.0005)),2.)/pow(0.001226695,2))+(pow(xc[1],2.)/pow(0.001165361,2))<1.)
                        /*set volume fraction to 1*/
                        {
                                C_VOF(cell,cell_thread)=1.;
                                count=count+1;
                        }
                        else
                        /*set volume fraction to 0*/
                        {
                                C_VOF(cell,cell_thread)=0.;
                        }
             }
             end_c_loop_all(cell,cell_thread)
          }
          printf("Number of cells of zirconium domain at the time of initialization is
: %d\n", count);
          }
        }
}
```

MATLAB VIDEO PROCESSING CODE

```
%%
%To get area of single phase drop
%Read video file and number of frames
path=('') %Enter video path
name=('.mpeg'); %Enter video name
video = VideoReader(strcat(path, name));
no_of_frames = video.NumberOfFrames;

%timescale
time_step= ; %Enter time step here
time=(0:no_of_frames-1)*time_step;

for m=1:no_of_frames
    %if mod(m,100)==0
        m
    %end
    image = read(video,m);
    image = rgb2gray(image); %convert to gray scale
    %image = image(20:600,331:575); %when the drop is vertical
    image = image(167:465,181:779); %when the drop is horizontal
```

```
    s=size(image); %get sizeof trimmed imagee
    count = 0; %initialize counter to zero
    for i=1:s(1,1)
        for j=1:s(1,2)  %2 for loops to chcek each pixel of matrix
            %if image(i,j)<29    %for the experiment video analysis
            if image(i,j)>29 && image(i,j)<80
                count=count+1;
            end
        end
    end
    area(m)=count;
end

% %To plot area vs simulation time
% plot(time,area)
% xlabel('Time')
% ylabel('Area')


%Frequency spectrum
four_tran=abs(fft(area-mean(area)));
sam_freq=length(area)/max(time);
freq=0:(sam_freq/length(area))+0.00001:sam_freq;

token = strtok(strcat(path,name),'.');
save(strcat(token,'.mat'));

%plots

subplot(1,2,1)
plot(time,area,'black','LineWidth',2)
xlabel ('Time (seconds)','FontSize', 25);
ylabel ('Amplitude (Number of pixels)','FontSize', 25);
title('Oscillation')
subplot(1,2,2)
plot(freq,four_tran,'black','LineWidth',2)
xlabel('Frequency (Hertz)', 'FontSize', 25)
ylabel('Amplitude (a.u.)', 'FontSize', 25)
axis([0,1000,0,1.2*max(four_tran)])
title('Frequency spectrum')

orient portrait
set(gcf, 'PaperPositionMode', 'manual', 'PaperUnits',
'inches','PaperPosition', [0 0 16 9]);
set(gcf,'PaperType','C');
%saveas (gcf, strcat(token,'.png'));
```

GENERATE .histo FILE

```
path = '';%Enter video path
video_name = '';%Enter video name without the extension
filename = strcat(path, video_name);
video_file = strcat(filename, '.mpeg'); %Select the extension
histo_file = strcat(filename, '.histo');
video=VideoReader(video_file); %enter video path here
```

```
num_frames = video.NumberOfFrames;
timestep = 5e-6*10;

%Write tag to the file
%Theory guide
https://www.mathworks.com/help/matlab/matlab_external/working-with-
pointers.html
tag = 'ESL Viscosity analysis histo file 18aug00 rwh
';
%tag = 'ESL Viscosity analysis histo file 18aug00 rwh
';
vp = libpointer('voidPtr',[int8(tag) 0]);
buffer_tag=vp.value;
outfile = fopen(histo_file,'w+');
nbytes_tag = fprintf(outfile,'%s',buffer_tag)
fclose(outfile);

%Write frequency
%Write data to a binary file:
https://www.mathworks.com/help/matlab/ref/fwrite.html
frequency = 1/timestep;
%frequency = 1000;
outfile = fopen(histo_file,'a+');
nbytes_frequency = fwrite(outfile,frequency,'double','l')
fclose(outfile);

%Write number of frames
num_frames;
outfile = fopen(histo_file,'a+');
nbytes_frames = fwrite(outfile,num_frames,'long','l')
fclose(outfile);

%Write histogram information
i = 1;
for i=1:num_frames
    i
         image = read(video,i);
         image = rgb2gray(image);
         %image = image(20:600,331:575); %when the drop is vertical
         image = image(167:465,181:779); %when the drop is horizontal
         [counts, ~] = imhist(image);
         %histo = transpose(counts);
         histo = counts;
         histo_record(i,:) = histo;
         %plot(histo);
         %hold on
         outfile = fopen(histo_file,'a+');
         nbytes_histo(i) = fwrite(outfile,histo,'long','l');
         fclose(outfile);
end
```

BIBLIOGRAPHY

[1] I. Egry, "Surface tension measurements of liquid metals by the oscillating drop tecnhique," *Journal of Materials Science*, vol. 26, pp. 2997-3003, 1991.

[2] R. Sangiorgi, G. Caracciolo, and A. Passerone, "Factors limiting the accurcy of measurements of surface tension by the sessile drop method," *Journal of Materials Science*, vol. 17, pp. 2895-2901, 1982.

[3] I. Egry, "The oscillation spectrum of compound drop," *Journal of Materials Science*, vol. 40, pp. 2239-2234, 2005.

[4] J. W. S. Rayleigh, "On the capillary phenomena of jets," *Proceedings of the Royal Society of London*, vol. 29, pp. 71-79, 1879.

[5] I. Egry, L. Ratke, M. Kolbe, D. Chatain, S. Curiotto, L. Battezzati, *et al.*, "Interfacial properties of immiscible Co-Cu alloys," *Journal of Materials Science*, vol. 45, pp. 1979-1985, 2010.

[6] J. Zhao, J. Lee, R. Wunderlich, H. Fecht, S. Schneider, M. SanSoucie, *et al.*, "Influence of oxygen on surface tension of zirconium," 2016.

[7] A. F. CFD. http://www.ansys.com/products/fluids/ansys-fluent.

[8] T. Iida and R. I. L. Guthrie, "The physical properties of liquid metals," ed: Oxford University Press Inc., New York, 1993.

[9] R. W. Hyers, "Modelling of and exoeriments on electromagnetic levitation for materials processing," Doctor of Philosophy, Materials Engineering, Massachusetts Institute of Technology, Cambridge, 1998.

[10] W. H. Reid, "The oscillations of a viscous liquid drop," *Quarterly of Applied Mathematics*, vol. 18, pp. 86-89, 1960.

[11] P. V. R. Suryanarayana and Y. Bayazitoglu, "Surface tension and viscosity from damped free oscillations of viscous droplets," *International Journal of Thermophysics*, vol. 12, pp. 137-151, 1991.

[12] M. Saffren, D. Ellmann, and W. K. Rhim, "Normal modes of compound drop," in *Second International Colloquium on Drops and Bubbles*, Monterey, California, 1981, p. 7.

[13] M. E. Frazer, W. K. LU, A. E. Hamielec, and R. Murarka, *Metallurgical and Materials Transactions*, vol. 2, 1971.

[14] J. Schade, A. McLean, and W. A. Miller, "Undercooled alloy phases," *Proceedings of the 115th Annual Meeting of TMS-AIME*, p. 233, 1986.

[15] B. J. Keene, K. C. Milla, A. Kasama, A. McLean, and W. A. Miller, *Metallurgical and Materials Transactions*, vol. B17, 1986.

[16] M. Watanabe, "Study of interfacial phenomena between liquid iron and slag system by using electrostatic furnace (ELF) on ISS," *10th Japan-Korea joint seminar on space environment utilization research (Korea university, Seoul, Korea,* September 12-13 2013.

[17] S. Watanabe, M. Amatatu, and T. Saito, "Densities of Fe-Ni, Co-Mo and Co-W aloys in liquid state," *Transactions of Japan Institute of Metals*, vol. 12, pp. 337-342, 1971.

[18] S. Watanabe and T. Saito, "Densities of Binary Copper Based Alloys in Liquid State," *Transactions of Japan institute of Metals and Materials*, vol. 13, pp. 186-191, 1972.

[19] R.-A. Eichel and I. Egry, "Surface tension and surface segregation of liquid cobalt-iron and cobalt-copper alloys," *Zeitschrift für Metallkunde,* vol. 90, pp. 371-375, 1999.
[20] R. W. Hyers, "Fluid flow effects in levitated droplets," *Measurement Science and Technology,* vol. 16, p. 8, 2005.
[21] S. Quan and D. P. Schmidt, "A moving mesh interface tracking method for 3D incompressible two-phase flows," *Journal of Computational Physics,* pp. 761-780, 2007.
[22] S. R. Berry, "Numerical simulationn of internal flow in electromagnetically-levitated liquid metal droplets," vol. Master of Science, 1998.
[23] M. Dai, J. B. Perot, and D. P. Schmidt, "Direct interface tracking of droplet deformation," *Atomizations and sprays,* 2002.
[24] R. Nallapati and J. B. Perot, "Numerical simulation of free-surface flows using a moving unstructured mesh," in *ASME FEDSM,* 2000.